

Towards Enhanced Recovery and System Stability: Analytical Solutions for Dynamic Incident Effects in Road Networks

Wenwei Yue¹, Student Member, IEEE, Changle Li², Senior Member, IEEE,
Shangbo Wang³, Member, IEEE, Zhigang Xu⁴, Member, IEEE,
and Guoqiang Mao, Fellow, IEEE

Abstract—Traffic incidents are recognized as a key contributor to non-recurrent congestion, which causes many negative effects in economy, environment, health and lifestyle. In this article, we investigate an incident management policy considering both signal control and route choice, which presents a real-time systematic effort to provide a rapid recovery from an incident and mitigate incident-related congestion according to different incident effects. Firstly, we introduce a route choice method on a multiple-route urban road network with consideration of bottleneck delays. Then, we analyze the route travel costs under incident effects and give the equilibrium existence condition after the occurrence of an incident. Furthermore, combining with the route choice method, a novel traffic signal control policy is proposed and the condition for equilibrium existence is given with the consideration of dynamic signal control and route choice simultaneously. Sufficient conditions for the dynamic road system to be stable are also derived and validated by using Lyapunov stability theorem. The analytical results indicate that opposite signal control policies should be applied in road networks under different incident circumstances and the proposed control policy can achieve the improved recovery rate and system stability than existing control policies in terms of dynamic incident effects in road networks. Finally, numerical results have been conducted to demonstrate the effectiveness of our proposed incident control policy and confirm the conditions for road system stability when different incident circumstances had been identified.

Index Terms—Incident management, route choice, traffic signal control, equilibrium existence, system stability.

I. INTRODUCTION

TRAFFIC incidents are notorious for the delay caused to road travelers, which accounts for one-quarter of all congestion on U.S. roadways approximately [1], and every minute that a lane is blocked leads to a 4-minute delay on the

average [2]. These incidents such as accidents, stalled vehicles and spilled loads often reduce roadway capacity, increase the potential for additional secondary incidents and generate negative effects on economy, environment and even people's health [3].

To mitigate these negative effects, traffic incident management policies are adopted by transportation authorities worldwide. According to an urban transportation report in 2007, reducing incident-related congestion saved 129.5 million hours and \$2493 million in 272 U.S. urban areas [4]. Most existing traffic incident management techniques in urban road networks are based on incident detection [5]–[9], incident duration estimation [10], [11] and incident signal control [12]–[14]. Firstly, a variety of methods have been utilized for incident detection, such as video camera based methods [5], artificial intelligence [6], vehicular networks [7], [8] and even social media based approaches [9]. These methods help to reduce the time between incident occurrence and its detection, which provide traffic participants with early warnings and accident rescue to mitigate negative effects of an incident. As another widely used incident management method, incident duration estimation can be utilized to provide travelers with timely traffic information and implement appropriate route guidance and diversion to mitigate the negative effects of non-recurrent congestion [10], [11]. However, these incident management methods only provide travelers with auxiliary traffic information to avoid the potential congestion, which cannot yield a real-time effective control policy to regulate the traffic flow and mitigate incident-related congestion dynamically based on different incident effects.

As an important and effective traffic control strategy, traffic signal control has been widely applied, and plays an indispensable role in managing road traffic flows and conflicting requirements, particularly in urban traffic networks. Optimization of traffic signals can alleviate congestion and reduce travel time of vehicles, which is also seen as an effective way to mitigate the negative incident effects and increase the road capacity. Long *et al.* [12] developed a signal control strategy and demonstrated its effectiveness in dispersing incident-based traffic jams in a two-way rectangular grid network. In [13], Huang *et al.* designed a traffic signal control systems based on Timed Petri nets (TPNs) to provide emergency vehicles with

Manuscript received March 4, 2020; revised June 17, 2020; accepted July 20, 2020. Date of publication August 4, 2020; date of current version December 28, 2021. This work was supported by the National Key Research and Development Program of China under Grant No. 2019YFB1600100. The Associate Editor for this article was G. Guo. (Corresponding author: Changle Li.)

Wenwei Yue, Changle Li, and Guoqiang Mao are with the State Key Laboratory of Integrated Services Networks, Xidian University, Xi'an 710071, China (e-mail: wenwei.yue@stu.xidian.edu.cn; clli@mail.xidian.edu.cn; g.mao@ieee.org).

Shangbo Wang is with the Institute of Transport and Logistic Studies (H73), The University of Sydney Business School, Sydney, NSW 2006, Australia (e-mail: shangbo.wang@sydney.edu.au).

Zhigang Xu is with the School of Information Engineering, Chang'an University, Xi'an 710064, China (e-mail: xuzhigang@chd.edu.cn).

Digital Object Identifier 10.1109/TITS.2020.3012307

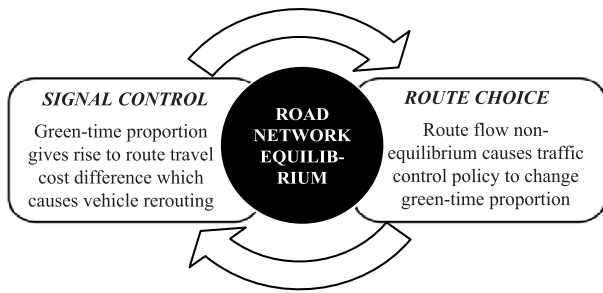


Fig. 1. An illustration of the relationship between route choice and signal control.

the highest priority, which can guarantee high speed and safety of these vehicles to reduce incident clearance time and improve traffic safety. Qi *et al.* [14] also adopted Petri nets (PNs) to design a traffic signal control system at an incident intersection and its upstream intersections, which helped to reduce incident-induced congestion and improved the real-time traffic incident management at intersections. It should be noted that in the aforementioned literature, traffic flows or route choice strategies are considered to be fixed when incident happens or traffic signal control policies change. However, as depicted in Figure 1, route choice and traffic signal control often interact with each other [15]. For example, route flow non-equilibrium may cause the traffic control policy to change the green-time proportion; such changes in turn give rise to changing route travel cost, which further causes vehicles to change routes, and the traffic network will be stable *if and only if* route choice and traffic signal control can reach an equilibrium simultaneously [15]. Moreover, there always exist a number of routes for each traveler from the origin to destination in urban road networks and the way that travelers choose their routes under incidents is different from the choices made under normal conditions. Therefore, when we propose a signal control policy to mitigate incident-induced congestion, both the route choice method and the signal control policy should be considered and analyzed. In summary, few existing works modeled the interactions between route choice and traffic signal control under incident effects and investigated the conditions for equilibrium existence and system stability.

To fill the gap, this article models the urban traffic system under incident conditions considering both route choice and signal control. The main emphases here are 1) to explore the interactions between route choice and signal control when an incident had been identified; and 2) to develop a responsive signal control policy to improve the stability of road systems under different incident circumstances. First, we introduce a route choice method on a multiple-route network and present an extension to further embrace bottleneck delays. Then, we analyze the route travel costs with incident effects using queueing theory and give the condition for the existence of a new Wardrop equilibrium in the event of an incident. Finally, a novel signal control policy incorporating the route choice method is proposed under different incident circumstances in road networks. The conditions for equilibrium existence and system stability under these policies are investigated.

Numerical results and discussions are also presented in this article which demonstrate the effectiveness of our proposed signal control policy in improving the recovery rate and the system stability of road network under incidents. More specifically, the following contributions are made in this article:

- the traffic flow swap between multiple routes in a road network is modeled considering the effect of an incident and a condition is given that the road network can recover to a new Wardrop equilibrium state after the occurrence of an incident;
- with joint consideration of the route choice method, a novel traffic signal control policy is proposed to mitigate the negative effects of an incident, which can better capture the interaction between route choice and traffic signal control under incident circumstances, and improve the recovery rate and the stability of road network systems with incidents;
- based on the proposed control policy, the condition for the existence of a new equilibrium after an incident is given and the stability of the road network system is proved by using Lyapunov stability theorem;
- analytical and numerical results demonstrate that opposite signal control policies should be utilized in road systems under different incident circumstances. If there is a minor incident that a new equilibrium exists in the original feasible region, the green-time proportion of the link with an incident should be increased to improve the convergence speed of dynamic road systems; and if there is a serious incident that a new equilibrium exists outside the original feasible region, the green-time proportion of the incident link should be decreased to enhance the recovery opportunity of road systems from a serious incident and improve the system stability with random disturbance.

The rest of the article is outlined as follows: Section II reviews related works. Section III introduces a route choice model with bottleneck delays in a general road network. Section IV analyzes the impact of incidents on traffic flow routing and gives the conditions that the road network can recover to a new equilibrium after an incident. In Section V, with the joint consideration of the route choice method, we propose a traffic signal control policy under incident effects, give the conditions for the existence of Wardrop equilibrium and prove the stability of the road network system. Section VI provides the numerical results to verify our theoretical findings. Section VII concludes the article.

II. RELATED WORK

Wardrop and Whitehead [16] proposed the idea of traffic equilibrium although the main idea dates back a long time ago, which suggested that under equilibrium conditions traffic arranges itself in congested networks such that all used routes between an Origin-Destination (OD) pair have equal and minimal costs, while all unused routes have greater or equal costs. The equilibrium notion is relevant to many dynamic systems and it is natural to seek such dynamical systems which have some realism [17]. In [18], Lin *et al.* applied a macroscopic fundamental diagram (MFD) to develop the existence

of network traffic flow equilibrium. Chen and Hu [19] focused on the equilibrium considering the interaction between signal setting and traffic assignment. Day-to-day traffic assignment model is believed to be the most appropriate for analyzing traffic equilibrium [20]. He *et al.* [20] proposed a day-to-day traffic assignment model based on link flow variables, which captured travelers' cost-minimization behavior in their travel path as well as their inertia. Zhao *et al.* [21] utilized day-to-day traffic assignment models to capture the rerouting reactions of travelers to advanced information and analyzed the stability of an equilibrium for the dynamic evolution of traffic costs and flows. Moreover, as a simple and intuitive traffic assignment model, the proportional switch adjustment process (PAP) has been widely used and extended to model day-to-day traffic flow dynamics [15], [17], [20]–[23], due to its intrinsic advantages: 1) traffic flow switches from a higher cost path to a lower cost path which is consistent with the individual travel behavior pursuing the least cost; 2) the concise mathematical structure and intuitive route adjustment behaviors enable PAP model to become versatile for the more complex road networks and many traffic assignment problems. Smith *et al.* developed the PAP dynamic traffic assignment model and proposed a P0 control policy considering a day-to-day route choice and traffic signal control. They showed that the P0 policy can move stage green time and converge to a certain equilibrium with vertical queueing [15] and also maximize network throughput at a quasi-dynamic user equilibrium [22]. In [23], Wang *et al.* applied PAP to model traffic flow swaps and green-time proportion changes for a dynamic traffic system and investigated conditions for the existence of equilibrium incorporating flow divergence in a network. Smith and Mounce [17] proposed a day-to-day rerouting model with the combination of signal control, which was shown to converge to the set of approximate consistent equilibrium under certain conditions.

Recently, various sensing techniques (*e.g.*, inductive loop detectors, video cameras and advanced on-board electronic devices) are more widely applied in traffic networks and provide travelers with the real-time traffic information for their current optimal rerouting, which allows the day-to-day model to be utilized within a day and helps to evaluate Intelligent Transportation Systems (ITS) interventions in the short term [17]. In this case, the day-to-day model has the potential to be used under incident condition and to investigate the user equilibrium when an incident had been identified, if fast computation can be completed online or previously calculated timings could be quickly downloaded [15]. More importantly, the notion of equilibrium provides promising opportunities for both short-term and long-term incident control in urban traffic networks. Specifically, a new equilibrium will exist during a long-term incident using the day-to-day model and the throughput of a road network is maximized at an user equilibrium [22], which improves traffic capacity under a long-term incident condition; on the other hand, even if an equilibrium may not exist during a short-term incident, when traffic flow swaps tend to an equilibrium, traffic capacity in a network will still be improved [22], [23].

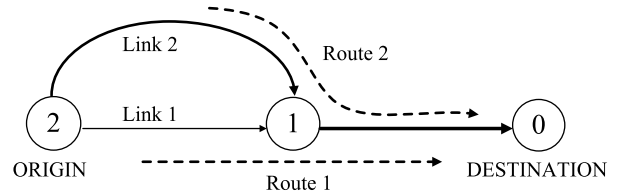


Fig. 2. A two route network.

To our knowledge, there are very few works investigating the existence condition of equilibrium and system stability under different incident conditions considering the interactions between route choice and traffic signal control.

III. ROUTE CHOICE METHOD WITH BOTTLENECK DELAY

The proportional switch adjustment process is viewed as (perhaps) the most natural route swapping process. It has simple mathematical structure and intuitive route adjustment behavior rule; in addition, PAP explicitly addresses the original micro-mechanism of network traffic evolution between multiple routes connecting the same OD pair. In this section, we firstly introduce the route choice method and then extend the PAP model to incorporate bottleneck delays using a $M/G/1$ queueing model with periodic vacations.

A. The Proportional Switch Traffic Flow Adjustment Process

Consider the simple network in Figure 2 and let $X_1(t)$ be the flow on route 1 at time t (vehicles per second); $X_2(t)$ be the flow on route 2 at time t (vehicles per second); s_1 be the saturation flow on link 1 (vehicles per second); s_2 be the saturation flow on link 2 (vehicles per second); $C_1(X_1(t))$ be the travel cost via route 1 at time t (seconds); $C_2(X_2(t))$ be the travel cost via route 2 at time t (seconds); $\mathbf{X}(t) = [X_1(t), X_2(t)]$ be the route flow vector at time t ; $\mathbf{C}(\mathbf{X}(t)) = [C_1(X_1(t)), C_2(X_2(t))]$ be the route-cost vector at time t .

Consider a fixed demand T (vehicles per second) so that $X_1(t) + X_2(t) = T$. More generally, the traffic flow on routes 1 and 2 should satisfy $\mathbf{D} = \{(X_1(t), X_2(t)) : X_1(t) + X_2(t) = T, X_1(t) \geq 0, X_2(t) \geq 0\}$. Following Wardrop equilibrium, we shall say that the traffic flow $\mathbf{X}(t)$ is in equilibrium if and only if more costly routes are not used [15]. Mathematically, suppose that at a specific time instant t , $C_1(X_1(t)) < C_2(X_2(t))$, and then the traffic flow $\mathbf{X}(t)$ is in equilibrium if and only if

$$X_2(t)[C_2(X_2(t)) - C_1(X_1(t))] = 0. \quad (1)$$

For a non-equilibrium flow $\mathbf{X}(t)$, it suggests that travelers may swap from route 2 to route 1 at time t at a rate $X_2(t)[C_2(X_2(t)) - C_1(X_1(t))]$ [15], which is an increasing function of both

- the flow $X_2(t)$ on the more expensive route 2 at time t ; and
- the difference $C_2(X_2(t)) - C_1(X_1(t))$ in route costs at time t .

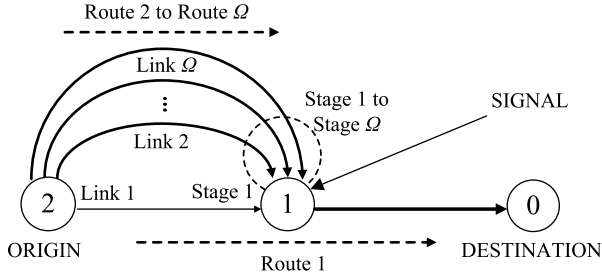


Fig. 3. A multiple-route signalized road network.

Hence with a suitable step length $w > 0$ [24], the changes $\Delta_1(\mathbf{X}(t))$, $\Delta_2(\mathbf{X}(t))$ in the traveler flows on routes 1 and 2 will be given by the following equations, respectively:

$$\Delta_1(\mathbf{X}(t)) = wX_2(t) [C_2(X_2(t)) - C_1(X_1(t))]; \quad (2)$$

$$\Delta_2(\mathbf{X}(t)) = -wX_2(t) [C_2(X_2(t)) - C_1(X_1(t))]. \quad (3)$$

Letting $[C_2(X_2(t)) - C_1(X_1(t))]_+ = \max\{C_2(X_2(t)) - C_1(X_1(t)), 0\}$, for the more general situation that $C_2(X_2(t))$ is not necessarily greater than $C_1(X_1(t))$, the notations in (2) and (3) become:

$$\Delta_1(\mathbf{X}(t)) = -wX_1(t) [C_1(X_1(t)) - C_2(X_2(t))]_+ + wX_2(t) [C_2(X_2(t)) - C_1(X_1(t))]_+; \quad (4)$$

$$\Delta_2(\mathbf{X}(t)) = -wX_2(t) [C_2(X_2(t)) - C_1(X_1(t))]_+ + wX_1(t) [C_1(X_1(t)) - C_2(X_2(t))]_+. \quad (5)$$

Let $\Delta_{12} = [-1, 1]$ and $\Delta_{21} = [1, -1]$, where Δ_{12} is a vector indicating a swap from route 1 to route 2 vector and Δ_{21} is a vector indicating a swap from route 2 to route 1 vector. Then, $\Delta(\mathbf{X}(t)) = [\Delta_1(\mathbf{X}(t)), \Delta_2(\mathbf{X}(t))]$ can be represented as

$$\Delta(\mathbf{X}(t)) = wX_1(t) [C_1(X_1(t)) - C_2(X_2(t))]_+ \Delta_{12} + wX_2(t) [C_2(X_2(t)) - C_1(X_1(t))]_+ \Delta_{21}. \quad (6)$$

Recall that $\mathbf{X}(t) = [X_1(t), X_2(t)]$, the dynamic system for the road network in Figure 2 can be represented as

$$\mathbf{X}(t+1) = \mathbf{X}(t) + \Delta(\mathbf{X}(t)). \quad (7)$$

B. Extending Route Choice Method to Incorporate Bottleneck Delays With Vertical Queueing

Considering a more general signalized road network in Figure 3, there is a traffic signal at node 1. Let G_i be the green-time proportion at the exit of link i and for all the Ω routes, the green-time proportion should be in set of $\mathbf{F} = \{\mathbf{G} : \sum_{i=1}^{\Omega} G_i = 1, G_i \geq 0\}$ and extending the demand set \mathbf{D} to a more general network with Ω routes, $\mathbf{D} = \{\mathbf{X} : \sum_{i=1}^{\Omega} X_i = T, X_i \geq 0\}$. Moreover, considering the capacity of each route, there should be a supply-feasible set $\mathbf{S} = \{(X_1, X_2, \dots, X_{\Omega}, G_1, G_2, \dots, G_{\Omega}) : X_1 \leq s_1 G_1, X_2 \leq s_2 G_2, \dots, X_{\Omega} \leq s_{\Omega} G_{\Omega}\}$ [15]. Therefore, the traffic flow and green-time proportion should belong to the set $\mathbf{D} \times \mathbf{F} \cap \mathbf{S}$ [15].

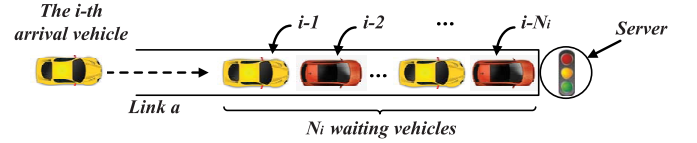


Fig. 4. Representation of a server and queue at an intersection.

Bottleneck delays at the exit of each link will affect the traffic flows and traffic costs on all routes, which must be accounted for in the cost vector \mathbf{C} already discussed above, and the total cost (running cost plus cost due to bottleneck delay) will then be felt by the route flow vector $\mathbf{X}(t)$. Also, the bottleneck delays will be affected by route flows. Thus, considering the bottleneck delays of all routes explicitly, we need to model this dynamical system in a way similar to the PAP dynamical system above. In this subsection, we utilize queueing theory to analyze the bottleneck delays with vertical queueing considering the random arrival of vehicles at a link. For a link with traffic signal, the vehicle queues can be modeled as a $M/G/1$ queue with periodic vacations [25]. At the green period of a traffic signal, vehicles leave the intersection gradually, which can be considered as vehicles receiving services at the exit of a link.

Definition 1 (Vertical Queueing): The vertical queue assumption presumes that vehicles on a roadway do not back up along the roadway, which would be considered a horizontal queue, but rather stack up upon one another at the point where congestion begins or at the stop line of a traffic signal. The vertical queueing assumption enables many calculations to be simplified and allows researchers to get to the core of their problem, while ignoring the effects of queue buildup on a roadway.

As shown in Figure 4, for link a , assume the service time of the k -th vehicle is S_k . When the i -th vehicle reaches the exit of a link, if there is a vehicle already in service, the waiting time of the i -th vehicle can be represented as

$$W_i = R_i + \sum_{k=i-N_i}^{i-1} S_k, \quad (8)$$

where R_i is the residual service time of the current vehicle being serviced (unfinished work expressed as the time needed to discharge the work). Otherwise, if when the i -th vehicle reaches the exit of a link, the server is idle (i.e., the system is empty), then $R_i = 0$. Parameter N_i is the (random) number of vehicles in the queue.

Therefore, the mean waiting time of a vehicle is

$$E\{W\} = E\{R_i\} + E\left\{\sum_{k=i-N_i}^{i-1} S_k\right\}. \quad (9)$$

The service time of each vehicle can be seen approximately as a constant $\frac{1}{s_a}$, where s_a is the saturation flow at the exit of link a . So (9) can be presented as

$$E\{W\} = E\{R_i\} + \frac{1}{s_a} \cdot E\{N_i\}. \quad (10)$$

As shown in (6) and (7), the traffic flow swaps proportionally between multiple routes at each time interval and the traffic flow during a time interval can be considered to be static. Thus by Little's law, the mean queue length $E\{N_i\}$ can be expressed in terms of the waiting time [26], [27]:

$$E\{N_i\} = x_a E\{W\}, \quad (11)$$

where x_a is the traffic flow rate of a link.

Substituting (11) into (10), the mean waiting time W can be presented as

$$E\{W\} = \frac{E\{R\}}{1 - \rho}, \quad (12)$$

where $\rho = \frac{x_a}{s_a}$.

Let $M(t)$ be the number of arrivals in the interval $(0, t)$, $L(t)$ be the number of vacation intervals in the interval $(0, t)$, S_i be the service time of the i -th vehicle, and V_i be the i -th vacation time. So the time average of $r(t)$ over $(0, t)$ can be presented as

$$\begin{aligned} \frac{1}{t} \int_0^t r(\tau) d\tau &= \frac{1}{t} \sum_{i=1}^{M(t)} \frac{1}{2} S_i^2 + \frac{1}{t} \sum_{i=1}^{L(t)} \frac{1}{2} V_i^2 \\ &= \frac{1}{2} \frac{M(t)}{t} \frac{\sum_{i=1}^{M(t)} S_i^2}{M(t)} + \frac{1}{2} \frac{L(t)}{t} \frac{\sum_{i=1}^{L(t)} V_i^2}{L(t)}, \end{aligned} \quad (13)$$

where $\frac{M(t)}{t}$ is the average vehicle arrival rate in the interval $(0, t)$, $\frac{L(t)}{t}$ is the vacation (red signal) arrival rate in the interval $(0, t)$, $\frac{\sum_{i=1}^{M(t)} S_i^2}{M(t)}$ is the second moment of S_i in the interval $(0, t)$, and $\frac{\sum_{i=1}^{L(t)} V_i^2}{L(t)}$ is the second moment of V_i in the interval $(0, t)$. As $t \rightarrow \infty$, the average residual service time $E\{R\}$ is

$$E\{R\} = \lim_{t \rightarrow \infty} \frac{1}{t} \int_0^t r(\tau) d\tau = \frac{1}{2} x_a \overline{S^2} + \frac{1}{2} \theta_a \overline{V^2}, \quad (14)$$

where θ_a is the the vacation (red signal) arrival rate at link a . Letting T_{cl} be the cycle length for a complete traffic signal cycle, then θ_a equals $\frac{1}{T_{cl}}$. Moreover, as mentioned before, the service time of each vehicle at the exit of link a is a constant $\frac{1}{s_a}$, which is determined by the link saturation flow. Also, the vacation time of traffic signal on link a is $(1 - G_a)T_{cl}$, which is determined by the cycle length for a complete traffic signal cycle T_{cl} and the green time proportion G_a on link a . Hence the mean residual service time $E\{R\}$ in (14) can be written as

$$E\{R\} = \frac{x_a}{2s_a^2} + \frac{(1 - G_a)^2 T_{cl}}{2}. \quad (15)$$

Substituting (15) into (12), the mean waiting time W is

$$E\{W\} = \frac{E\{R\}}{1 - \rho} = \frac{x_a}{2s_a(s_a - x_a)} + \frac{s_a(1 - G_a)^2 T_{cl}}{2(s_a - x_a)}. \quad (16)$$

And the mean sojourn time b_a (bottleneck delays) of a vehicle at link a can be presented as

$$b_a = E\{W\} + \frac{1}{s_a} = \frac{2s_a + s_a^2(1 - G_a)^2 T_{cl} - x_a}{2s_a(s_a - x_a)}. \quad (17)$$

Equation (17) involves link flows, which are connected to route flows via the route-link incidence matrix \mathbf{A} . This matrix is defined as follows:

$$A_a = \begin{cases} 1, & \text{if link } a \text{ is part of the route} \\ 0, & \text{otherwise} \end{cases}. \quad (18)$$

Then, $x_a = (\mathbf{A}\mathbf{X})_a$, (17) becomes:

$$b_a = \frac{2s_a + s_a^2(1 - G_a)^2 T_{cl} - (\mathbf{A}\mathbf{X})_a}{2s_a(s_a - (\mathbf{A}\mathbf{X})_a)}. \quad (19)$$

Let \mathbf{b} be the vector of bottleneck delays of links, which can be written as

$$\mathbf{b} = [b_1, b_2, \dots, b_{N_l}], \quad (20)$$

where N_l is the number of links in the road network. Then, $(\mathbf{A}^T \mathbf{b})_i$ can be seen as the total bottleneck delay of the i -th route.

Thus by extending the proportional switch rerouting dynamic system in (7) with two routes to incorporate bottleneck delays with vertical queueing in (19, 20), the change $\Delta(\mathbf{X}(t))$ in (6) can be written as

$$\begin{aligned} \Delta(\mathbf{X}(t)) &= wX_1[C_1(X_1(t)) + (\mathbf{A}^T \mathbf{b})_1 \\ &\quad - C_2(X_2(t)) - (\mathbf{A}^T \mathbf{b})_2]_+ \Delta_{12} \\ &\quad + wX_2[C_2(X_2(t)) + (\mathbf{A}^T \mathbf{b})_2 \\ &\quad - C_1(X_1(t)) - (\mathbf{A}^T \mathbf{b})_1]_+ \Delta_{21}. \end{aligned} \quad (21)$$

As shown in Figure 3, (21) can be extended to a more general network with multiple routes between a single OD pair. Denote by $r \sim h$ if routes r and h join the same OD pair, and then the traffic flow swap between routes r and h is:

$$\begin{aligned} \Delta(\mathbf{X}(t)) &= \sum_{\{(r,h):r < h\}} w\{X_r[C_r(X_r(t)) + (\mathbf{A}^T \mathbf{b})_r \\ &\quad - C_h(X_h(t)) - (\mathbf{A}^T \mathbf{b})_h]_+ \Delta_{rh} \\ &\quad + X_h[C_h(X_h(t)) + (\mathbf{A}^T \mathbf{b})_h \\ &\quad - C_r(X_r(t)) - (\mathbf{A}^T \mathbf{b})_r]_+ \Delta_{hr}\}. \end{aligned} \quad (22)$$

According to [15], (22) may then be readily extended to the case where there are several routes joining several OD pairs, by putting, for OD pair q :

$$\begin{aligned} \Delta_{\text{OD}q}(\mathbf{X}(t)) &= \sum_{\{(r,h):r < h\}} w\{X_{qr}[C_{qr}(X_{qr}(t)) + (\mathbf{A}^T \mathbf{b})_{qr} \\ &\quad - C_{qh}(X_{qh}(t)) - (\mathbf{A}^T \mathbf{b})_{qh}]_+ \Delta_{qrh} \\ &\quad + X_{qh}[C_{qh}(X_{qh}(t)) + (\mathbf{A}^T \mathbf{b})_{qh} \\ &\quad - C_{qr}(X_{qr}(t)) - (\mathbf{A}^T \mathbf{b})_{qr}]_+ \Delta_{qhr}\}. \end{aligned} \quad (23)$$

For all the K OD pairs, the traffic flow swap is $\Delta(\mathbf{X}) = [\Delta_{\text{OD}1}(\mathbf{X}), \Delta_{\text{OD}2}(\mathbf{X}), \dots, \Delta_{\text{OD}K}(\mathbf{X})]$.

The extended proportional switch rerouting dynamic system also can be written as:

$$\mathbf{X}(t+1) = \mathbf{X}(t) + \Delta(\mathbf{X}(t)). \quad (24)$$

The stability of system with proportional switch rerouting method has been studied in [15], which refers to asymptotic stability [28], [29]. Specifically, under suitable condition (route cost C is monotone and smooth, and is an increasing function of route flow X , which is proved in Section IV), the system asymptotically converges to an equilibrium. However, in [15], bottleneck delays have not been considered in route cost C . In this article, as shown in (19), the bottleneck delay is also an increasing function of route flow X in the set of $\mathbf{D} \times \mathbf{F} \cap \mathbf{S}$. Hence the dynamic system in (24) with bottleneck delays can also converge to an equilibrium.

IV. INCIDENT EFFECT ON ROUTE TRAFFIC FLOW

With the development of advanced sensing techniques, traffic information such as link flows, travel speed and even incidents can be monitored timely. Using the real-time information, many studies have been proposed to investigate incident duration estimation [10], [11] considering multiple influential factors of traffic incidents, such as incident type, number of lanes and traffic volume by using machine learning and artificial intelligence. In this case, when an incident had been identified, the real-time traffic costs for routes between the same OD pair can be estimated and informed neighboring vehicles to provide real-time road conditions for their future route planning. Note that the driver compliance has been considered in PAP route choice model. Specifically, when an incident occurred, a number of drivers at routes with the incident tend to reroute and choose the path with lower travel cost, which is consistent with the individual travel behavior pursuing the least cost. Even if other drivers choose to remain on the routes with incidents, according to the Wardrop equilibrium [16], all the routes between the same OD pair tend to have the same travel costs gradually and the real-time traffic information provided by advanced sensing techniques can efficiently promote the convergence of road network system in a short term. In this section, we first analyze the traffic flow swaps in an urban road network interrupted by incidents using queueing theory. Then, considering the average travel delays with incidents on road links, we extend the dynamic system in (24). Finally, we give the existence condition for a new Wardrop equilibrium after an incident and prove the stability of the dynamic system.

A. Extending the Route Choice Method to Incorporate Link Costs With Incident Effects

When using queueing theory to analyze the travel cost of a link with incident, the space occupied by a vehicle on a link can be seen as a “server”, which starts service as soon as a vehicle enters the link and conducts the “service” until the end of the link is reached [26], [27] and the service rate is related to the average travel speed and the length of the link. Hence, for each link, the number of servers, m , is limited, which is determined by the multiplication of jam density, length of the road link, and the number of lanes. Moreover, assuming that the vehicle arrival process can be modeled by a Poisson process with an arrival rate x_a and the service time is exponentially distributed [30] with service rate μ .

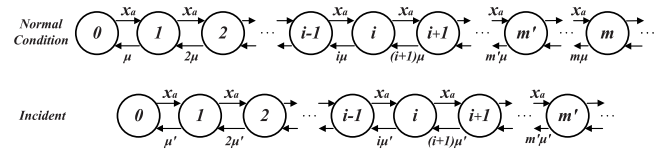


Fig. 5. State transition diagram under normal and incident conditions.

Vehicle arrival process on a link without incident can be modeled by a $M/M/m$ queueing system. However, as soon as an incident occurs, both the number of working servers and service rates of all servers decrease until the incident is cleared. During the incident, the number of servers decreases from m to $m' \leq m$ and the service rates of all servers drop from μ to $\mu' \geq 0$. Hence the queueing process under normal and incident conditions can be modeled as two $M/M/m$ queueing system with different service rate and number of servers, as shown in Figure 5. Note that the number of servers m' and service rate μ' under incident condition can be estimated with consideration of multiple incident influential factors (*e.g.*, traffic flow, incident type, number of lanes, vehicle lane-changing and weaving maneuvers) by artificial intelligence [10], [11] to calculate link travel costs under different incident conditions.

Let the steady-state probability of the state that i vehicles are on the link under normal condition be P_i and the steady-state equilibrium equations can be written as:

$$\begin{cases} x_a P_{i-1} = i \mu P_i, & i \leq m \\ x_a P_{i-1} = m \mu P_i, & i > m. \end{cases} \quad (25)$$

Then, we can get the expressions of all steady-state probability P_i

$$P_i = \begin{cases} P_0 \frac{(m\eta)^i}{i!}, & i \leq m \\ P_0 \frac{m^m \eta^i}{m!}, & i > m, \end{cases} \quad (26)$$

where $\eta = \frac{x_a}{m\mu} < 1$. Using the fact $\sum_{i=0}^{\infty} P_i = 1$, we have

$$P_0 = \left[1 + \sum_{i=1}^{m-1} \frac{(m\eta)^i}{i!} + \sum_{i=m}^{\infty} \frac{(m\eta)^i}{m!} \frac{1}{m^{i-m}} \right]^{-1}. \quad (27)$$

Hence the number of vehicles awaiting services can be written as

$$N_Q = \sum_{i=0}^{\infty} i P_{i+m} = \frac{P_0 (m\eta)^m}{m!} \sum_{i=0}^{\infty} i \eta^i = \frac{P_0 (m\eta)^m}{m!} \frac{\eta}{(1-\eta)^2}. \quad (28)$$

Using the Little's law, the expected running time of a link under normal condition can be represented as

$$c_N = \frac{1}{\mu} + \frac{N_Q}{x_a} = \frac{1}{\mu} + \frac{1}{x_a} \cdot \frac{P_0 (m\eta)^m}{m!} \frac{\eta}{(1-\eta)^2}. \quad (29)$$

Similarly, the expected running time of a link under incident condition is

$$c_I = \frac{1}{\mu'} + \frac{N_Q}{x_a} = \frac{1}{\mu'} + \frac{1}{x_a} \cdot \frac{(m'\eta')^{m'}}{m'!} \frac{\eta'}{(1-\eta')^2} \cdot \left[1 + \sum_{i=1}^{m'-1} \frac{(m'\eta')^i}{i!} + \sum_{i=m'}^{\infty} \frac{(m'\eta')^i}{m'!} \frac{1}{m'^{i-m'}} \right]^{-1}, \quad (30)$$

where $\eta' = \frac{x_a}{m'\mu'} < 1$. In summary, the average running time on link a under normal and incident condition can be written as:

$$c_a = \begin{cases} \frac{1}{\mu} + \frac{1}{x_a} \frac{P_0(m\eta)^m}{m!} \frac{\eta}{(1-\eta)^2}, & \text{under normal condition} \\ (30), & \text{under incident condition.} \end{cases} \quad (31)$$

Based on the route-link incidence matrix \mathbf{A} in (18) and traffic flow on link a , $x_a = (\mathbf{A}\mathbf{X})_a$, (31) can be rewritten into (32), shown at the bottom the page.

Let the vector of average travel time of links be $\mathbf{c} = [c_1, c_2, \dots, c_L]$ and let $(\mathbf{A}^T\mathbf{c})_i$ be the travel time of the i -th route. Then, the traffic flow swap at each OD pair in (23) considering incident effects can be written as:

$$\begin{aligned} \Delta_{\text{ODq}}(\mathbf{X}(t)) &= \sum_{\{(r,h):r<h\}} w\{X_{qr}\} \left[(\mathbf{A}^T(\mathbf{c} + \mathbf{b}))_{qr} \right. \\ &\quad - (\mathbf{A}^T(\mathbf{c} + \mathbf{b}))_{qh}]_+ \Delta_{qrh} + X_{qh} \left[(\mathbf{A}^T(\mathbf{c} + \mathbf{b}))_{qh} \right. \\ &\quad \left. - (\mathbf{A}^T(\mathbf{c} + \mathbf{b}))_{qr}]_+ \Delta_{qhr}. \end{aligned} \quad (33)$$

The dynamic system considering incident effects is the same as that in (24).

B. Equilibrium Existence and System Stability Under Incident Effects

After an incident occurring on a link, the travel cost of this link increases from $c_N(x(t))$ to $c_I(x(t))$ with the subscripts N and I denoting normal and incident conditions respectively. Let the total costs of the i -th routes under normal condition at time t be $C_{Ni}(X_i(t)) = (\mathbf{A}^T(\mathbf{c}_N + \mathbf{b}))_i$ and let the total costs of the i -th routes under incident condition at time t be $C_{Ii}(X_i(t)) = (\mathbf{A}^T(\mathbf{c}_I + \mathbf{b}))_i$. Then, for all k routes including the incident link, the travel costs will be increased from $\mathbf{C}_N = \{C_{N1}(X_1(t)), C_{N2}(X_2(t)), \dots, C_{Nk}(X_k(t))\}$ to $\mathbf{C}_I = \{C_{I1}(X_1(t)), C_{I2}(X_2(t)), \dots, C_{Ik}(X_k(t))\}$, respectively. Thus for route i including the incident link, assuming

that an incident occurs at time t^* , and letting $C_{Ii}(X_\delta) = C_{Ni}(X_i(t^*))$, then we can obtain the extra route flow $\Delta X_i = X_i(t^*) - X_\delta$, which leads to a non-equilibrium in the dynamic system due to incident effects. However, for the route j without including the incident link, the extra route flows $\Delta X_j = 0$. In this way, for all Ω routes in the road network, the extra route flow vector is $\Delta \mathbf{X}_R = \{\Delta X_1, \Delta X_2, \dots, \Delta X_\Omega\}$. The total extra route flow is

$$\Delta X_T = \sum_{i=1}^{\Omega} \Delta X_i. \quad (34)$$

Hence if the dynamic system achieves equilibrium again, the total extra route flow ΔX_T should be allocated to all routes between the same OD pair according to their travel cost expressions. Using this system of equations in (35), we can obtain the extra flows on all routes that cause the dynamic system returning to a new equilibrium after incident effects:

$$\begin{cases} \Delta X_{I1} + \Delta X_{I2} + \dots + \Delta X_{I\Omega} = \Delta X_T \\ (\mathbf{A}^T(\mathbf{c} + \mathbf{b}))_1(\Delta X_{I1}) = (\mathbf{A}^T(\mathbf{c} + \mathbf{b}))_2(\Delta X_{I2}) \\ = \dots = (\mathbf{A}^T(\mathbf{c} + \mathbf{b}))_\Omega(\Delta X_{I\Omega}) \end{cases} \quad (35)$$

where Ω is the number of routes between an OD pair. In this way, letting the vector of extra route flows $\Delta \mathbf{X}_I$ after an incident be $\{\Delta X_{I1}, \Delta X_{I2}, \dots, \Delta X_{I\Omega}\}$, the dynamic system can reach a new equilibrium $\mathbf{X}_1^* = \mathbf{X}(t^*) - \Delta \mathbf{X}_R + \Delta \mathbf{X}_I$ if and only if this equilibrium still belongs to the set $\mathbf{D} \times \mathbf{F} \cap \mathbf{S}$. In the rest of this subsection, we will give the equilibrium existence and system stability conditions and prove them respectively.

1) *Equilibrium Existence*: We first give the existence condition of equilibrium in the set $\mathbf{D} \times \mathbf{F} \cap \mathbf{S}$, if $\mathbf{D} \times \mathbf{F} \cap \mathbf{S}$ is non-empty.

Theorem 2: For the dynamic system formulated in (24), a road network stays in an equilibrium state before the occurrence of an incident. Assuming that an incident occurs at time t^* , let the vector of route flow when an incident occurs be $\mathbf{X}(t^*)$, and then if the route flow vector meets the condition that for each $\mathbf{X}_0 \in \mathbf{D} \times \mathbf{F} \cap \mathbf{S} \setminus \mathbf{B}$ (\mathbf{B} is the boundary of the non-empty set $\mathbf{D} \times \mathbf{F} \cap \mathbf{S}$), there is a positive real number $k < 1$, when $\mathbf{X} \in \mathbf{D} \times \mathbf{F} \cap \mathbf{S} \setminus (\mathbf{D} \times \mathbf{F} \cap \mathbf{kS})$, such that $-\mathbf{C}_E(\mathbf{X}) \cdot (\mathbf{X}_0 - \mathbf{X}) > \mathbf{0}$, then there is a new Wardrop equilibrium $\mathbf{X}(t^*) - \Delta \mathbf{X}_R + \Delta \mathbf{X}_I \in \mathbf{D} \times \mathbf{F} \cap \mathbf{S}$.

Proof: This proof is given in Appendix A. ■

2) *System Stability*: In order to prove the stability of the proposed dynamic system, we first state the definition of system stability and the Lyapunov stability theorem [31].

$$c_a = \begin{cases} \frac{1}{\mu} + \frac{\left(\frac{(\mathbf{A}\mathbf{X})_a}{\mu}\right)^m \cdot \frac{(\mathbf{A}\mathbf{X})_a}{m\mu}}{(\mathbf{A}\mathbf{X})_a \cdot m! \cdot \left(1 - \frac{(\mathbf{A}\mathbf{X})_a}{m\mu}\right)^2} \cdot \left[1 + \sum_{i=1}^{m-1} \frac{\left(\frac{(\mathbf{A}\mathbf{X})_a}{\mu}\right)^i}{i!} + \sum_{i=m}^{\infty} \frac{\left(\frac{(\mathbf{A}\mathbf{X})_a}{\mu}\right)^i}{m! \cdot m^{i-m}} \right]^{-1}, & \text{under normal condition} \\ \frac{1}{\mu'} + \frac{\left(\frac{(\mathbf{A}\mathbf{X})_a}{\mu'}\right)^{m'} \cdot \frac{(\mathbf{A}\mathbf{X})_a}{m'\mu'}}{(\mathbf{A}\mathbf{X})_a \cdot m'! \cdot \left(1 - \frac{(\mathbf{A}\mathbf{X})_a}{m'\mu'}\right)^2} \cdot \left[1 + \sum_{i=1}^{m'-1} \frac{\left(\frac{(\mathbf{A}\mathbf{X})_a}{\mu'}\right)^i}{i!} + \sum_{i=m'}^{\infty} \frac{\left(\frac{(\mathbf{A}\mathbf{X})_a}{\mu'}\right)^i}{m'! \cdot m'^{i-m'}} \right]^{-1}, & \text{under incident condition} \end{cases} \quad (32)$$

Definition 3: The dynamic system is stable if and only if, starting from any point $X_0 \in \mathbf{D} \times \mathbf{F} \cap \mathbf{S}$, the system in (24) converges to an equilibrium as $t \rightarrow +\infty$.

Theorem 4 (Lyapunov Stability Theorem): Let $\Delta(\mathbf{X}(t))$ be continuously differentiable. Then, the dynamic system in (24) is stable if there is a continuously differentiable scalar function $V(\cdot)$, defined throughout the set $\mathbf{D} \times \mathbf{F} \cap \mathbf{S}$, such that

- $V(\mathbf{X}) \geq 0$ for all $\mathbf{X} \in \mathbf{D} \times \mathbf{F} \cap \mathbf{S}$;
- $V(\mathbf{X}) = 0$ if and only if \mathbf{X} is an equilibrium; and
- $\text{grad } V(\mathbf{X}) \cdot \Delta(\mathbf{X}(t)) < 0$ if \mathbf{X} is not an equilibrium.

According to Definition 3 and Theorem 4, we first present a candidate Lyapunov function V based on the dynamic system in (24) under incident condition, which can be written as

$$V_q(\mathbf{X}(t)) = \sum_{\{(r,h):r<h\}} w\{X_{qr}\{[(\mathbf{A}^T(\mathbf{c}+\mathbf{b}))]_{qr} - (\mathbf{A}^T(\mathbf{c}+\mathbf{b}))_{qh} \}_+ \Delta_{qrh}\}^2 + X_{qh}\{[(\mathbf{A}^T(\mathbf{c}+\mathbf{b}))]_{qh} - (\mathbf{A}^T(\mathbf{c}+\mathbf{b}))_{qr} \}_+ \Delta_{qhr}\}^2. \quad (36)$$

$$V(\mathbf{X}(t)) = \sum_q V_q(\mathbf{X}(t)). \quad (37)$$

Theorem 5: After an incident, if the new Wardrop equilibrium $\mathbf{X}(t^*) - \Delta\mathbf{X}_R + \Delta\mathbf{X}_I \in \mathbf{D} \times \mathbf{F} \cap \mathbf{S}$, then for any starting point $X_0 \in \mathbf{D} \times \mathbf{F} \cap \mathbf{S}$, the dynamic system in (24) is stable.

Proof: For all $\mathbf{X} \in \mathbf{D} \times \mathbf{F} \cap \mathbf{S}$, it is easy to see that $V(\mathbf{X}) \geq 0$. If the new Wardrop equilibrium is in the set $\mathbf{D} \times \mathbf{F} \cap \mathbf{S}$, then there must be an equilibrium such that $V(\mathbf{X}) = 0$. Moreover, the function V also satisfies $\text{grad } V(\mathbf{X}) \cdot \Delta(\mathbf{X}(t)) < 0$ if \mathbf{X} is not an equilibrium, the proof of which is given in Appendix B. ■

So $V(\mathbf{X}(t))$ is a Lyapunov function for the dynamic system (24) and if a new Wardrop equilibrium $\mathbf{X}(t^*) - \Delta\mathbf{X}_R + \Delta\mathbf{X}_I \in \mathbf{D} \times \mathbf{F} \cap \mathbf{S}$, then the dynamic system (24) under incident is stable.

V. TRAFFIC SIGNAL CONTROL POLICY

With the increasing applications of Advanced Traveler Information Systems (ATIS) (e.g., inductive loop detectors, video cameras, warning lights and advanced on-board electronic devices) [32], dynamic route guidance service can provide the real-time traffic information for drivers, which enables traffic flows to be readily monitored and analyzed. More importantly, the real-time traffic information helps travelers choose the current optimal route, which allows the day-to-day model to be utilized within a day and helps to evaluate ITS interventions in the short term [17]. Based on existing studies about short-term incident control [12]–[14], [33], a traffic signal control system for an incident intersection has been presented in Figure 6, where many kinds of sensors are installed at an intersection to capture and provide real-time traffic information for travelers. For instance, inductive loop detectors are applied to collect traffic volume and average travel speed and cameras are adopted to detect the type and severity of an incident. These traffic data can be transmitted to an Information Processing Center (IPC) to estimate traffic costs on the incident link and then provide travelers with

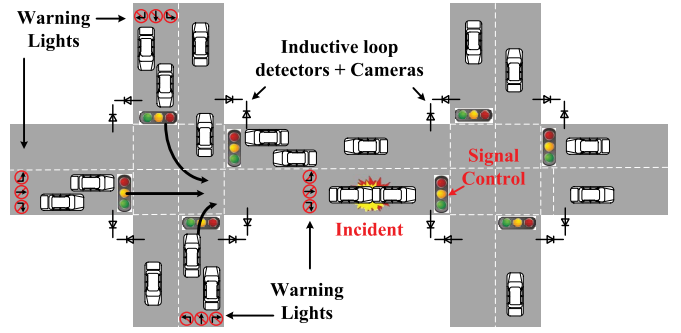


Fig. 6. Traffic signal control system at an intersection.

rerouting guidance for their future routes via the roadside warning lights. Moreover, combining the proportional vehicle rerouting method, in this section, we propose a novel traffic signal control policy to adjust the green-time proportion for traffic signal at downstream of the incident area,¹ as illustrated in Figure 6, which implements different control strategies according to the severity of an incident and achieves a more rapid recovery rate and an increased stability of the road system under incident conditions.

Specifically, considering the road network in Figure 3, there is a traffic signal at node 1. For convenience, we still utilize a two-route network with signals to illustrate our proposed signal control policy, but for further system model and equilibrium analysis, we use a more general network with multiple routes in Figure 3. According to the rerouting method, the road network can achieve an equilibrium \mathbf{X}^* before the occurrence of an incident. However, if an incident occurs on route 2 suddenly, the total travel cost of route 2 will be increased such that $C_{E1}(\mathbf{X}^*) < C_{E2}(\mathbf{X}^*)$ at the former equilibrium \mathbf{X}^* and the dynamic system cannot maintain the stability at this route flow vector \mathbf{X}^* any more. Thus in order to achieve a new equilibrium and recover road network from an incident, according to the proportional switch rerouting method, traffic flow will be swapped from route 2 to route 1 gradually and if there is a new equilibrium \mathbf{X}_1^* in the feasible region $\mathbf{D} \times \mathbf{F} \cap \mathbf{S}$ such that $C_{E1}(\mathbf{X}_1^*) = C_{E2}(\mathbf{X}_1^*)$, the dynamic system can reach a new equilibrium to recover from an incident. However, if a new equilibrium \mathbf{X}_1^* is not in the feasible region $\mathbf{D} \times \mathbf{F} \cap \mathbf{S}$ based on the constant green-time proportion, the system cannot reach a new equilibrium to recover from an incident. Moreover, an increased recovery rate should also be considered in the implementation of the traffic control policy.

Therefore, considering traffic signal control and combining vehicle rerouting method with a proper signal control policy provides a promising way to achieve a better road network control after an incident. In this way, if both route traffic flow and the green-time proportion of traffic signal can achieve an equilibrium $[\mathbf{X}^*, \mathbf{G}^*]$ simultaneously, the dynamic system

¹For an extended road network with many traffic signals at the intersections among multiple OD pairs, we can adjust the green-time proportion for traffic signal at destination of the OD pair with an incident. In this case, the proposed signal control policy can relieve incident-induced congestion and improve recovery rate from an incident for the OD pair.

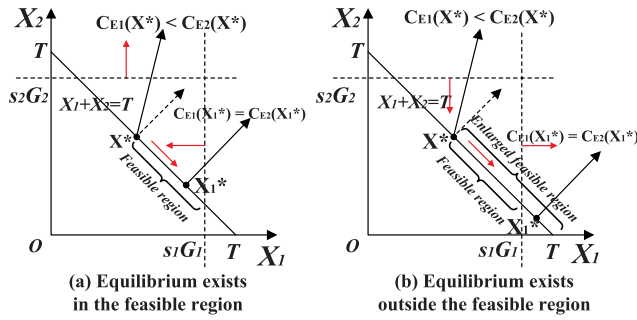


Fig. 7. An illustration of signal control policy under incident condition.

can be stable. After an incident, according to the equilibrium existence condition in Theorem 2, we can calculate the new route flow equilibrium \mathbf{X}_1^* . Based on the instant green-time proportion, if there is a minor incident in a road network and the route flow equilibrium \mathbf{X}_1^* exists in the feasible region, as illustrated in Figure 7(a), then we can reduce the green-time proportion G_1 on route 1 and increase the green-time proportion G_2 on route 2. Thus in combination with the route choice method in Section III, both the travel cost and bottleneck delay of route 2 will be reduced simultaneously and with a suitable length step, the dynamic system can achieve a new equilibrium $[\mathbf{X}_1^*, \mathbf{G}_1^*]$ eventually, which can lead to a quicker recovery of dynamic system to reach the new equilibrium \mathbf{X}_1^* and conduce to an improvement of the system recovery ability under incident condition. However, if there is a serious incident and a new route flow equilibrium \mathbf{X}_1^* exists outside the feasible region when an incident occurs, as shown in Figure 7(b), the feasible region should be enlarged appropriately to incorporate the new equilibrium $[\mathbf{X}_1^*, \mathbf{G}_1^*]$. In this case, we can increase the green-time proportion G_1 on route 1 and reduce the green-time proportion G_2 on route 2, as shown in Figure 7(b) and with a suitable step length, the dynamic system will reach the equilibrium $[\mathbf{X}_1^*, \mathbf{G}_1^*]$, which provides an increasing opportunity of road system recovery from an incident and improves the stability of traffic network with random disturbance. In summary, the proposed signal control policy can benefit road networks under both long-term and short-term incident conditions, due to that 1) for the long-term incidents, such as work zone closure, based on the day-to-day model in Section III, traffic flows in road networks can achieve a new equilibrium eventually using our proposed control strategy and the traffic capacity can be maximized during the long-term incident [22], [23]; 2) for the short-term incidents, such as accidents, an equilibrium may not be reached during the incident clearance, however, according to the analysis results in [22], [23], traffic capacity will be increased gradually when the dynamic system trends towards an equilibrium state, which is consistent with the control policy in this section, thus our proposed control strategies can also achieve a better performance in road network recovery and system stability under short-term incident conditions.

Mathematically, let $G_1(t)$ be the green-time proportion on route 1 on time t and $G_2(t)$ be the green-time proportion on route 2 on time t . If a new equilibrium \mathbf{X}_1^* exists in the feasible

region, with a suitable step length $w' > 0$, the green-time proportion change $\Delta G_1(t)$ and $\Delta G_2(t)$ on time t can be written as:

$$\Delta G_1(t) = -w'G_1(t)[C_{E2}(X_2(t)) - C_{E1}(X_1(t))]_+ + w'G_2(t)[C_{E1}(X_1(t)) - C_{E2}(X_2(t))]_+; \quad (38)$$

$$\Delta G_2(t) = -w'G_2(t)[C_{E1}(X_1(t)) - C_{E2}(X_2(t))]_+ + w'G_1(t)[C_{E2}(X_2(t)) - C_{E1}(X_1(t))]_+. \quad (39)$$

Let $\Delta_{rh} = \begin{bmatrix} 0, \dots, 0, \underbrace{-1}_{r-th}, 0, \dots, 0, \underbrace{1}_{h-th}, 0, \dots \end{bmatrix}$, $\Delta_{hr} = \begin{bmatrix} 0, \dots, 0, \underbrace{1}_{r-th}, 0, \dots, 0, \underbrace{-1}_{h-th}, 0, \dots \end{bmatrix}$ and $\Delta \mathbf{G}_{ODq}(t) = [\Delta G_{q1}(t), \Delta G_{q2}(t), \dots, \Delta G_{q\Omega}(t)]$ (Ω is the number of routes between an OD pair q). For a more general network with several routes between multiple OD pairs, the green-time proportion change at each OD pair is

$$\Delta \mathbf{G}_{ODq}(t) = \sum_{\{(r,h):r<h\}} w' \{G_{qr}(t)[C_{Eqh}(X_{qh}(t)) - C_{Eqr}(X_{qr}(t))]_+ \Delta_{qrh} + G_{qh}(t) \times [C_{Eqr}(X_{qr}(t)) - C_{Eqh}(X_{qh}(t))]_+ \Delta_{qhr}\}. \quad (40)$$

For all the K OD pairs, the green-time proportion change is

$$\Delta \mathbf{G}(t) = [\Delta \mathbf{G}_{OD1}(t), \Delta \mathbf{G}_{OD2}(t), \dots, \Delta \mathbf{G}_{ODK}(t)]. \quad (41)$$

Similarly, if a new equilibrium \mathbf{X}_1^* lies outside the feasible region, as shown in Figure 7(b), the green-time proportion change at each OD pair can be written as

$$\Delta \mathbf{G}_{ODq}(t) = \sum_{\{(r,h):r<h\}} w' \{G_{qh}(t)[C_{Eqh}(X_{qh}(t)) - C_{Eqr}(X_{qr}(t))]_+ \Delta_{qhr} + G_{qr}(t) \times [C_{Eqr}(X_{qr}(t)) - C_{Eqh}(X_{qh}(t))]_+ \Delta_{qrh}\}. \quad (42)$$

For all the K OD pairs, the green-time proportion change can also be written as (41).

Let $\mathbf{G}(t)$ be the green-time proportions on all the routes between multiple OD pairs and for both equilibrium existence circumstances above, the dynamic system governing green-time proportion can be written as

$$\mathbf{G}(t+1) = \mathbf{G}(t) + \Delta \mathbf{G}(t). \quad (43)$$

Combining the rerouting dynamic system in (24) and green-time proportion dynamic system in (43), we have

$$\Delta [\mathbf{X}, \mathbf{G}] = [\Delta \mathbf{X}(t), \Delta \mathbf{G}(t)]. \quad (44)$$

The traffic dynamic system considering both rerouting and traffic signal control can be written as

$$[\mathbf{X}, \mathbf{G}](t+1) = [\mathbf{X}, \mathbf{G}](t) + \Delta [\mathbf{X}, \mathbf{G}](t). \quad (45)$$

A. Equilibrium Existence

As illustrated in Figure 7, using the proposed traffic signal control policy, we can adjust the supply-feasible set \mathbf{S} dynamically according to the equilibrium existence conditions. Hence for each $\mathbf{G}_j(\mathbf{t}) = [G_{1j}(t), G_{2j}(t), \dots, G_{\Omega j}(t)]$ between an OD pair (Ω is the number of routes between the OD pair) belonging to $\mathbf{F} = \left\{ \mathbf{G} : \sum_{i=1}^{\Omega} G_i(t) = 1, G_i(t) \geq 0 \right\}$, there is a supply-feasible set $\mathbf{S}_j = \{(X_1, X_2, \dots, X_{\Omega}, G_{1j}, G_{2j}, \dots, G_{\Omega j}) : X_1 \leq s_1 G_{1j}, X_2 \leq s_2 G_{2j}, \dots, X_{\Omega} \leq s_{\Omega} G_{\Omega j}\}$ and the union of all the supply-feasible sets forms a larger supply-feasible set \mathbf{S}_T . Then, after an incident, if a new equilibrium exists in the demand-feasible set $\mathbf{D} \times \mathbf{F} \cap \mathbf{S}_T$, the system in (45) can reach an equilibrium eventually. In this case, considering both the traffic signal control and the route choice, we propose a new equilibrium existence condition as follows.

Theorem 6: For the dynamic system formulated in (45), if the route flow \mathbf{X} and green-time proportion \mathbf{G} meet the condition that if there is a $\mathbf{G}_j \subseteq \mathbf{F}$, for each $\mathbf{X}_0 \in \mathbf{D} \times \mathbf{F} \cap \mathbf{S}_j \setminus \mathbf{B}$, there is a positive real number $k < 1$, when $\mathbf{X} \in \mathbf{D} \times \mathbf{F} \cap \mathbf{S}_j \setminus (\mathbf{D} \times \mathbf{F} \cap k\mathbf{S}_j)$, such that $-\mathbf{C}_E(\mathbf{X}) \cdot (\mathbf{X}_0 - \mathbf{X}) > \mathbf{0}$, then there is a Wardrop equilibrium $[\mathbf{X}^, \mathbf{G}^*] \in \mathbf{D} \times \mathbf{F} \cap \mathbf{S}_T$.*

The key step of the proof of Theorem 6 is given in Appendix A. Compared with the existence condition in Theorem 2, when the condition in Theorem 6 is satisfied, the dynamic system in (45) using both rerouting and traffic signal control can enlarge the feasible region of equilibrium from $\mathbf{D} \times \mathbf{F} \cap \mathbf{S}_j$ to $\mathbf{D} \times \mathbf{F} \cap \mathbf{S}_T$, which provides the traffic system with a higher recovery ability from an incident and enhances the stability of road network significantly.

B. System Stability

Based on the dynamic system specified in (45), we first presented a function V considering both proportional switch rerouting method and traffic signal control policy. Then, using Definition 3 and Lyapunov stability theorem (Theorem 4), we propose conditions of system stability under different equilibrium existence conditions in Figure 14 and give the corresponding proofs.

The candidate Lyapunov function for the whole system is:

$$V([\mathbf{X}(\mathbf{t}), \mathbf{G}(\mathbf{t})]) = V(\mathbf{X}(\mathbf{t})) + V(\mathbf{G}(\mathbf{t})), \quad (46)$$

where

$$\begin{aligned} V_q(\mathbf{X}(\mathbf{t})) = & \sum_{\{(r,h):r<h\}} w\{X_{qr}\{(\mathbf{A}^T(\mathbf{c}+\mathbf{b}))_{qr} \\ & - (\mathbf{A}^T(\mathbf{c}+\mathbf{b}))_{qh}\}_{+} \Delta_{qrh}\}^2 + X_{qh}\{(\mathbf{A}^T(\mathbf{c}+\mathbf{b}))_{qh} \\ & - (\mathbf{A}^T(\mathbf{c}+\mathbf{b}))_{qr}\}_{+} \Delta_{qhr}\}^2. \end{aligned} \quad (47)$$

$$V(\mathbf{X}(\mathbf{t})) = \sum_q V_q(\mathbf{X}(\mathbf{t})). \quad (48)$$

For the circumstance that a new equilibrium exists in the feasible region, according to (40), $V(\mathbf{G}(\mathbf{t}))$ can be

written as

$$\begin{aligned} V_q(\mathbf{G}(\mathbf{t})) = & \sum_{\{(r,h):r<h\}} w'\{G_{qr}\{[C_{Eqh}(X_{Eqh}(\mathbf{t})) \\ & - C_{Eqr}(X_{qr}(\mathbf{t}))]_{+} \Delta_{qrh}\}^2 + G_{qh}\{[C_{Eqr}(X_{qr}(\mathbf{t})) \\ & - C_{Eqh}(X_{qh}(\mathbf{t}))]_{+} \Delta_{qhr}\}^2\}; \end{aligned} \quad (49)$$

$$V(\mathbf{G}(\mathbf{t})) = \sum_q V_q(\mathbf{G}(\mathbf{t})). \quad (50)$$

Similarly, for the circumstance that a new equilibrium exists outside the feasible region, according to (42), $V(\mathbf{G}(\mathbf{t}))$ is

$$\begin{aligned} V_q(\mathbf{G}(\mathbf{t})) = & \sum_{\{(r,h):r<h\}} w'\{G_{qh}\{[C_{Eqh}(X_{Eqh}(\mathbf{t})) \\ & - C_{Eqr}(X_{qr}(\mathbf{t}))]_{+} \Delta_{qhr}\}^2 + G_{qr}\{[C_{Eqr}(X_{qr}(\mathbf{t})) \\ & - C_{Eqh}(X_{qh}(\mathbf{t}))]_{+} \Delta_{qrh}\}^2\}; \end{aligned} \quad (51)$$

$$V(\mathbf{G}(\mathbf{t})) = \sum_q V_q(\mathbf{G}(\mathbf{t})). \quad (52)$$

Theorem 7: When an incident occurs, if an equilibrium $[\mathbf{X}^, \mathbf{G}^*]$ exists in the feasible region, using our proposed traffic signal control policy, the dynamic system specified in (45) will be stable. However, for the circumstance that an equilibrium $[\mathbf{X}^*, \mathbf{G}^*]$ exists outside the feasible region, the dynamic system (45) is stable if for each route i of all OD pairs, 1) $\frac{\partial C_{Ei}(X_i(t))}{\partial X_i(t)} + \frac{\partial C_{Ei}(G_i(t))}{\partial G_i(t)} > 0$; and 2) $wX_i > w'G_i$.*

Proof: Obviously, for all $\mathbf{X} \in \mathbf{D} \times \mathbf{F} \cap \mathbf{S}_T$, $V([\mathbf{X}(\mathbf{t}), \mathbf{G}(\mathbf{t})]) \geq 0$ and if and only if \mathbf{X} is a Wardrop equilibrium, $V([\mathbf{X}(\mathbf{t}), \mathbf{G}(\mathbf{t})]) = 0$. Moreover, the candidate Lyapunov function $V([\mathbf{X}(\mathbf{t}), \mathbf{G}(\mathbf{t})])$ should also satisfy $\frac{\partial V([\mathbf{X}(\mathbf{t}), \mathbf{G}(\mathbf{t})])}{\partial \mathbf{X}(\mathbf{t})} \cdot \Delta \mathbf{X}(\mathbf{t}) + \frac{\partial V([\mathbf{X}(\mathbf{t}), \mathbf{G}(\mathbf{t})])}{\partial \mathbf{G}(\mathbf{t})} \cdot \Delta \mathbf{G}(\mathbf{t}) < 0$, if $[\mathbf{X}(\mathbf{t}), \mathbf{G}(\mathbf{t})]$ is not an equilibrium. This proof is given in Appendix C. ■

Under the circumstance that an equilibrium $[\mathbf{X}^*, \mathbf{G}^*]$ exists outside the feasible region, according to the two conditions in Theorem 7, only when the total travel cost change caused by vehicle rerouting is larger than that caused by the green-time proportion change, the dynamic system (45) will be stable. This result is exactly consistent with Figure 7(b). In Figure 7(b), $C_{E1}(X_1) < C_{E2}(X_2)$ after an incident. Then, according to our proposed signal control policy, the green-time proportion of route 1 will increase and that of route 2 will decrease, which leads to an increase in the total travel cost on route 2. If the system can reach an equilibrium, the traffic flow on route 2 should swap to route 1 gradually such that $C_{E1}(X_1) = C_{E2}(X_2)$ eventually. In this way, the total travel cost change caused by the green-time proportion change should be less than that caused by vehicle rerouting. Thus the result suggests the effectiveness of our proposed control policy to improve the stability of road network after the occurrence of an incident.

VI. NUMERICAL RESULTS

The proposed dynamic system (45) is tested on an one-OD three-route road network, as illustrated in Figure 8. We can see that there are 3 routes from intersection 0 to 5, route 1 (intersection 0 \rightarrow 1 \rightarrow 2 \rightarrow 5), route 2 (intersection 0 \rightarrow 3 \rightarrow 2 \rightarrow 5) and route 3 (intersection 0 \rightarrow 3 \rightarrow 4 \rightarrow 5).

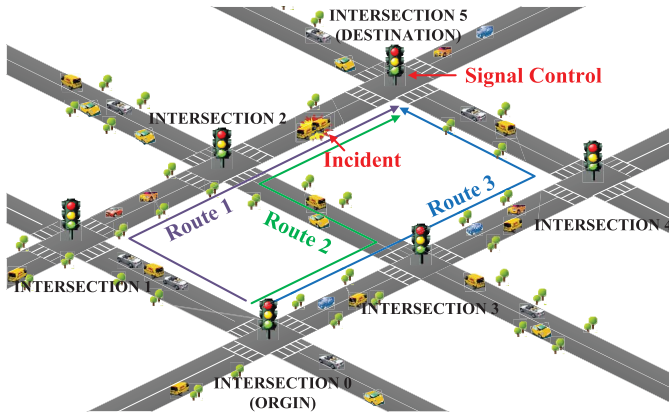


Fig. 8. The one-OD three-route road network.

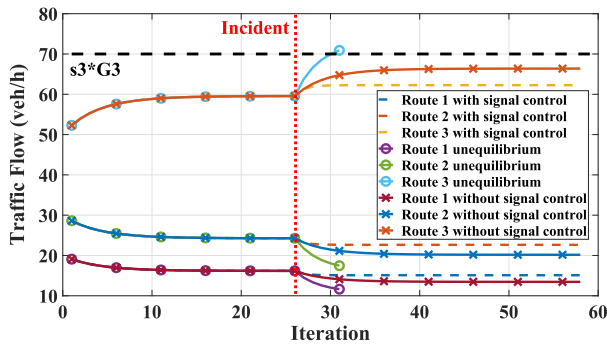


Fig. 9. Temporal evolution of traffic flows under different incident conditions.

When an incident had been identified on the link between intersection 2 and 5, the travel costs of route 1 and route 2 will increase and the traffic flows on these routes will also swap to route 3 gradually. In this case, we will adjust green-time proportions for the traffic signal at intersection 5 based on the proposed control policy to study the conditions for equilibrium existence and system stability under different incident scenarios.

For the one-OD three-route road network, we set the lengths of the three routes as 1 km, 1 km and 0.9 km and the saturation flows as 75 vehicles/h, 75 vehicles/h and 100 vehicles/h respectively. The free speed of all routes, the total demand and the duration of traffic light cycle are set to be 50 km/h, 100 vehicles/h and 120 seconds, respectively. The start point of traffic flows is set as $\mathbf{X}_0 = [20, 30, 50]$ and the start point for green-time proportions at intersection 5 is set as $\mathbf{G}_0 = [0.3, 0.7]$. The step length is set according to the rules proposed in [24].

First, when there are no incidents in the road network, traffic flows will switch from the route with a higher cost to a lower cost route. In this case, the road network can achieve an equilibrium, where travel costs of all the three routes are equal, only based on the route choice behavior of drivers. As shown in Figure 9, the dynamical system is stable and reaches an equilibrium point after approximately 20 iterations. Then, an incident occurs on the link between intersection 2 and 5, at the 26-th iteration and travel costs of route 1 (intersection $0 \rightarrow 1 \rightarrow 2 \rightarrow 5$) and route 2 (intersection $0 \rightarrow 3 \rightarrow 2 \rightarrow 5$)

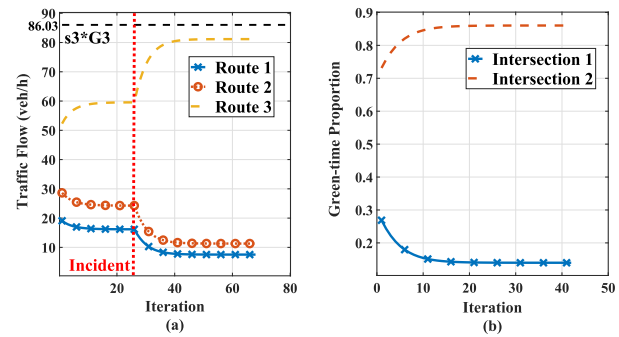


Fig. 10. Temporal evolution of traffic flows and green-time proportions if the condition for system stability is fulfilled.

will increase suddenly based on the analytical results in (32). In this case, as depicted in Figure 9, based on the route choice model in this article, traffic flows on route 1 and route 2 will swap to route 3 gradually. The outputs of the dynamical system under different incident conditions are given in Figure 9. If the condition for existence of equilibrium in Theorem 5 is satisfied, as illustrated by the solid line with cross marker, the dynamical system can achieve a new equilibrium after approximately 40 iterations. However, if the condition in Theorem 5 is not satisfied, for example, when there is a serious incident such that a new equilibrium exists outside the feasible region $\mathbf{D} \times \mathbf{F} \cap \mathbf{S}$, as illustrated by the solid line with circle marker, the traffic flow on route 3 reaches the boundary of the supply-feasible set $\mathbf{S} = \{(X_1, X_2, X_3, G_1, G_2, G_3) : X_1 \leq s_1 G_1, X_2 \leq s_2 G_2, X_3 \leq s_3 G_3\}$ and the dynamical system cannot approach a feasible equilibrium point [15].

Moreover, in Figure 9, we also give the temporal evolution of traffic flows using our proposed signal control policy for the circumstance that a new equilibrium exists in the feasible region and compare it with the method that utilizes route choice only. As illustrated by the dotted line, if an equilibrium still exists in the feasible region, the dynamical system using the route choice and signal control combined technique can achieve a new equilibrium after about 30 iterations, which is consistent with the condition in Theorem 7. More importantly, the dynamical system using our proposed control policy shows a quicker convergence speed, which suggests the superiority of our proposed control policy in improving the recovery rate of road networks from an incident, provided that there is a minor incident in road networks and a new equilibrium still exists in the feasible region.

As illustrated by the solid line with circle marker in Figure 9, when there is a serious incident such that a new equilibrium exists outside the feasible region, the dynamical system cannot reach a new equilibrium only using the route choice method. Under this circumstance, in this article, we propose a novel traffic signal control policy combined with the route choice model and give a sufficient condition for system stability, as shown in Theorem 7. Figure 10 illustrates the temporal evolution of traffic flows and green-time proportions if the condition in Theorem 7 is fulfilled. We can see that with the help of signal control, the boundary of the supply-feasible set increases from 70 to 86.03, which allows

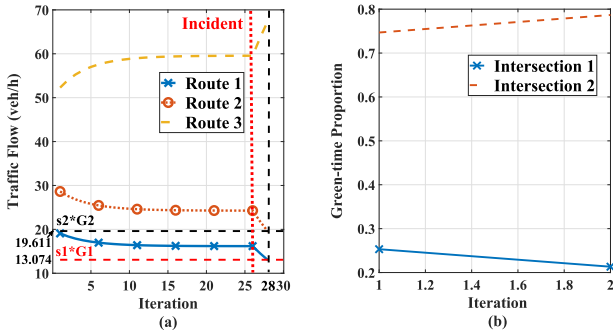


Fig. 11. Temporal evolution of traffic flows and green-time proportions if the condition for system stability is NOT fulfilled.

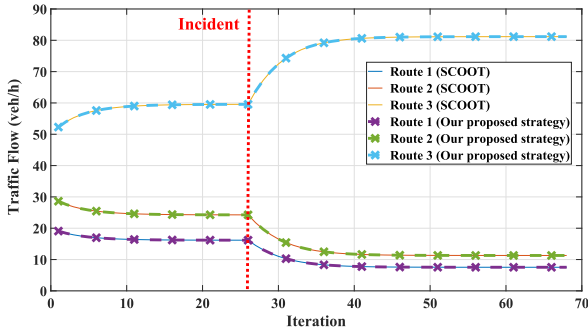


Fig. 12. Signal control based on SCOOT and our proposed strategy; a new equilibrium exists outside the feasible region.

the dynamic supply-feasible set to include a new equilibrium after an incident. However, if the condition in Theorem 7 is not fulfilled, as shown in Figure 11, the dynamical system cannot reach a feasible equilibrium point, which implies that traffic congestion will accumulate indefinitely and the traffic system will be unstable. In summary, according to our analysis and simulations, if a new equilibrium exists outside the feasible region, the green-time proportion of the routes with an incident should be increased to incorporate the new equilibrium in the feasible region. When the condition in Theorem 7 can be fulfilled, the road network can achieve stable after a serious incident. Therefore, the proposed control policy can provide an increased opportunity of road system recovery from an incident and improve the system stability with random disturbance.

As an effective actuated signal control strategy, Split, Cycle and Offset Optimization Technique (SCOOT) has been applied in many cities around world extensively and achieves reduced vehicle delays in these cities, which repeats in real time to make adjustments of splits, offsets, and cycle time in small steps based on the real-time vehicle volumes from the upstream links. In this article, we compare the proposed control strategy with SCOOT under the circumstance that a new equilibrium exists inside or outside the feasible region, respectively. For the circumstance that a new equilibrium exists outside the feasible region, as shown in Figure 12, if the conditions for system stability in Theorem 7 can be fulfilled, the dynamic system achieve a new equilibrium based on both SCOOT and our proposed strategy with the same convergence

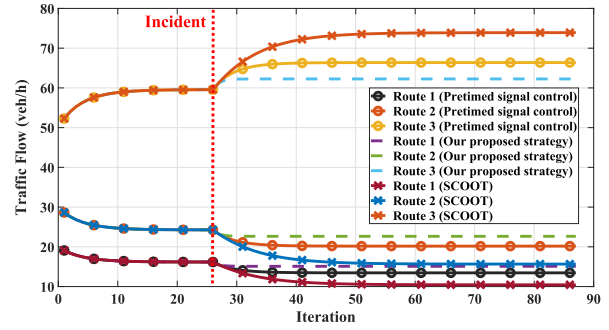


Fig. 13. Signal control based on SCOOT and our proposed strategy; a new equilibrium exists inside the feasible region.

speed, because the green-time proportion for routes with an incident will be decreased according to SCOOT, which is similar to our proposed control policy, as shown in Figure 7(b). However, for the circumstance that a new equilibrium exists in the feasible region, although the dynamical system can achieve a new equilibrium using SCOOT, their convergence speeds are different, as illustrated in Figure 13. We can see that our proposed control policy (dotted lines) allows the fastest convergence speed and the signal control based on SCOOT (solid lines with cross marker) has the slowest convergence speed, which is even slower than the pretimed signal control strategy (solid lines with circle marker), because the decrease of green-time proportion on routes with an incident will reduce the convergence speed of the dynamic system. While our proposed control policy will increase the green-time proportion for these routes, when there is a minor incident and a new equilibrium exists in the feasible region, which will increase the convergence speed and improve the recovery rate of the road network from an incident.

VII. CONCLUSION

In this article, we proposed an incident management policy considering the interactions between signal control and route choice, which exhibits a more rapid recovery rate from an incident and improves the stability of road network system under incidents. We first introduced a route choice model, *i.e.*, the proportional switch rerouting method, and extended this model to embrace incident effects. The condition for a new Wardrop equilibrium existence after an incident was also given. Then, a novel control policy was proposed, which can provide a real-time effective control to regulate the traffic flow and mitigate incident-related congestion based on different incident effects dynamically. We further gave the condition for Wardrop equilibrium existence considering both route choice and signal control, which showed that our proposed policy is superior in providing an increasing opportunity of road system recovery from an incident compared with existing signal control policies. A sufficient condition for the system stability was also derived and proved by using Lyapunov stability theorem. Finally, simulation results were conducted to verify our theoretical findings and demonstrate the effectiveness of the proposed incident control policy.

The theoretical results derived in this article indicated that if there is a minor incident in a road network and a new equilibrium still exists in the feasible region $\mathbf{D} \times \mathbf{F} \cap \mathbf{S}$, the road network can reach a new equilibrium gradually via the route choice of drivers only. However, if there is a serious incident and a new equilibrium exists outside the feasible region $\mathbf{D} \times \mathbf{F} \cap \mathbf{S}$, the system cannot achieve a new equilibrium only based on the drivers' route choice. Combining the route choice with signal control, the feasible region can be enlarged such that the system could become stable only when the conditions in Theorem 7 can be met. The theoretical results and the proposed control policy can be used to design an improved signal control policy to supplement the pure micro-model and to improve the state-of-the-art in real-time traffic incident management in urban traffic networks. In the future, for the possible applications in real networks, we intend to extend the proposed signal control policy incorporating more complex route choice model with multiple transportation modals. Moreover, for a more complex network where there are many intersections and traffic signals among multiple OD pairs, it will be interesting to investigate an optimal control policy with consideration of signal coordination at multiple intersections to further improve the network capacity under incident circumstances.

APPENDIX A PROOF OF THEOREM 3

In this appendix, we prove that if the route flow \mathbf{X} meets the condition in (24), then there is a new Wardrop equilibrium $\mathbf{X}(t^*) - \Delta \mathbf{X}_R + \Delta \mathbf{X}_I \in \mathbf{D} \times \mathbf{F} \cap \mathbf{S}$. Let $C_{Ei}(X_i(t)) = (\mathbf{A}^T(\mathbf{b} + \mathbf{c}))_i$ be the total travel cost of route i . Following Wardrop equilibrium, if there exists a new route flow equilibrium $\mathbf{X}_1^* = \mathbf{X}(t^*) - \Delta \mathbf{X}_R + \Delta \mathbf{X}_I$, then for all route flow $\mathbf{X} \in \mathbf{D} \times \mathbf{F} \cap \mathbf{S}$,

$$\mathbf{C}_E(\mathbf{X}_1^*) \cdot \mathbf{X} \geq \mathbf{C}_E(\mathbf{X}_1^*) \cdot \mathbf{X}_1^*, \quad (53)$$

which is equivalent to the following two conditions:

$$-\mathbf{C}_E(\mathbf{X}_1^*) \cdot (\mathbf{X} - \mathbf{X}_1^*) \leq 0, \quad (54)$$

and

$$-\mathbf{C}_E(\mathbf{X}_1^*) \text{ is normal at } \mathbf{X}_1^* \text{ to } \mathbf{D} \times \mathbf{F} \cap \mathbf{S}. \quad (55)$$

Because $\mathbf{C}_E(\mathbf{X})$ is monotonically increasing, for a road network in Figure 2 with two routes between an OD pair, the condition in Theorem 2 can be also written as Corollary 8.

Corollary 8: If there is $\mathbf{X}_1 \in \mathbf{D} \times \mathbf{F} \cap \mathbf{S}$, such that $C_{E1}(\mathbf{X}_1) > C_{E2}(\mathbf{X}_1)$ and there is also $\mathbf{X}_2 \in \mathbf{D} \times \mathbf{F} \cap \mathbf{S}$, such that $C_{E1}(\mathbf{X}_2) < C_{E2}(\mathbf{X}_2)$, then there exists a Wardrop equilibrium $\mathbf{X}_1^ \in \mathbf{D} \times \mathbf{F} \cap \mathbf{S}$.*

It is worth noting that, for convenience, we utilize a network with two routes between an OD pair as an illustration of equilibrium existence, as shown in Figure 14. The obtained results however can be readily extended to a general road network with multiple routes [15]. Moreover, for further theorems and proofs about the existence of equilibrium and system stability, we conduct them on a more general network with multiple routes in Figure 3.

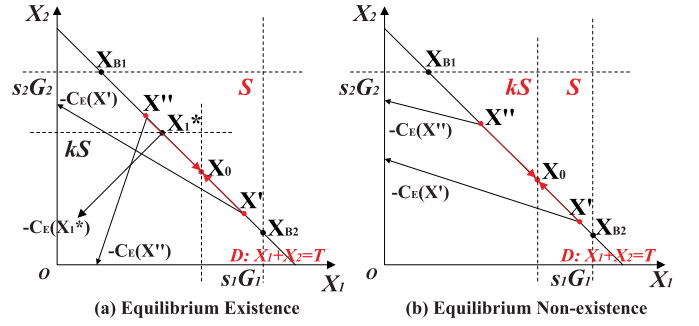


Fig. 14. An illustration of equilibrium existence in road network with two routes.

The illustrations of equilibrium existence and non-existence are shown in Figure 14(a) and Figure 14(b) respectively. In a network with two routes, the demand-feasible set is $\mathbf{D} = \{(X_1, X_2) : X_1 + X_2 = T, X_1 \geq 0, X_2 \geq 0\}$ and the supply-feasible set can be written as $\mathbf{S} = \{(X_1, X_2, G_1, G_2) : X_1 \leq s_1 G_1, X_2 \leq s_2 G_2\}$, as shown in Figure 14. Considering Figure 14(a) and assuming that there is a new equilibrium \mathbf{X}_1^* , according to the Wardrop equilibrium, $C_{E1}(\mathbf{X}_1^*) = C_{E2}(\mathbf{X}_1^*)$. For each $\mathbf{X}_0 \in \mathbf{D} \times \mathbf{F} \cap \mathbf{S} \setminus \mathbf{B}$, as shown in Figure 14(a), there exists a set of vectors \mathbf{X}' between \mathbf{X}_0 and \mathbf{X}_{B2} (on the boundary), such that $-\mathbf{C}_E(\mathbf{X}') \cdot (\mathbf{X}_0 - \mathbf{X}') > 0$. Meanwhile, there also exists a set of vectors \mathbf{X}'' between \mathbf{X}_0 and \mathbf{X}_{B1} (on the another boundary), such that $-\mathbf{C}_E(\mathbf{X}'') \cdot (\mathbf{X}_0 - \mathbf{X}'') > 0$. Hence in Figure 14(a), let $k = \max \left\{ \frac{1}{s_1 G_1} (\mathbf{X}_0)_1, \frac{1}{s_2 G_2} (\mathbf{X}_1^*)_2 \right\}$, where $(\mathbf{X}_0)_1$ is the traffic flow on route 1 of vector \mathbf{X}_0 and $(\mathbf{X}_1^*)_2$ is the traffic flow on route 2 of vector $(\mathbf{X}_1^*)_2$, and then for all $\mathbf{X} \in \mathbf{D} \times \mathbf{F} \cap \mathbf{S} \setminus (\mathbf{D} \times \mathbf{F} \cap k\mathbf{S})$, $-\mathbf{C}_E(\mathbf{X}) \cdot (\mathbf{X}_0 - \mathbf{X}) > 0$.

However, if there does not exist a new equilibrium $\mathbf{X}_1^* \in \mathbf{D} \times \mathbf{F} \cap \mathbf{S}$ after an incident, as shown in Figure 14(b), according to Corollary 8, for all $\mathbf{X} \in \mathbf{D} \times \mathbf{F} \cap \mathbf{S}$, $C_{E1}(\mathbf{X}) > C_{E2}(\mathbf{X})$ or $C_{E1}(\mathbf{X}) < C_{E2}(\mathbf{X})$. Then, for each $\mathbf{X}_0 \in \mathbf{D} \times \mathbf{F} \cap \mathbf{S} \setminus \mathbf{B}$, there only exists a set of vectors \mathbf{X} between \mathbf{X}_0 and one of boundary vector \mathbf{X}_{B1} or \mathbf{X}_{B2} , such that $-\mathbf{C}_E(\mathbf{X}) \cdot (\mathbf{X}_0 - \mathbf{X}) > 0$. In this case, we cannot find any $0 < k < 1$ that for all $\mathbf{X} \in \mathbf{D} \times \mathbf{F} \cap \mathbf{S} \setminus (\mathbf{D} \times \mathbf{F} \cap k\mathbf{S})$, such that $-\mathbf{C}_E(\mathbf{X}) \cdot (\mathbf{X}_0 - \mathbf{X}) > 0$.

In summary, if the traffic flow meets the condition that for each $\mathbf{X}_0 \in \mathbf{D} \times \mathbf{F} \cap \mathbf{S} \setminus \mathbf{B}$ (\mathbf{B} is the boundary of the non-empty set $\mathbf{D} \times \mathbf{F} \cap \mathbf{S}$), there is a positive real number $k < 1$, when $\mathbf{X} \in \mathbf{D} \times \mathbf{F} \cap \mathbf{S} \setminus (\mathbf{D} \times \mathbf{F} \cap k\mathbf{S})$, such that $-\mathbf{C}_E(\mathbf{X}) \cdot (\mathbf{X}_0 - \mathbf{X}) > 0$, then there is a Wardrop equilibrium $\mathbf{X}_1^* \in \mathbf{D} \times \mathbf{F} \cap \mathbf{S}$.

Theorem 2 is proved.

APPENDIX B PROOF OF THEOREM 6

In this appendix, we shall prove that $\text{grad } V(\mathbf{X}) \cdot \Delta(\mathbf{X}(t)) < 0$ for all non-equilibrium \mathbf{X} in $\mathbf{D} \times \mathbf{F} \cap \mathbf{S}$. Let $C_{Ei}(X_i(t)) = C_i(X_i(t)) + (\mathbf{A}^T \mathbf{b})_i$ be the total travel cost of route i .

Thus $\text{grad } V(\mathbf{X}) \cdot \Delta(\mathbf{X}(t))$ can be written as (56), shown at the bottom of the next page, where $\mathbf{1}_{qi} = [0, \dots, 0, \underbrace{1}_{i\text{-th}}, 0, \dots, 0]$.

It can be readily shown that the matrix \mathbf{J}_{qrh} is a semi-negative definite matrix, each $\Delta_{\text{ODq}}^{\text{T}}(\mathbf{X}(t)) \mathbf{J}_{\text{qrh}} \Delta_{\text{ODq}}(\mathbf{X}(t))$ is less than or equal to 0. As for each $\sum_{r,h,u} \{[C_{Eqr} - C_{Eqh}]_+^2 \cdot \{X_{qu}[C_{Equ} - C_{Eqr}]_+ - X_{qr}[C_{Eqr} - C_{Equ}]_+\}$, if and only if $C_{Equ} > C_{Eqr} > C_{Eqh}$, then there is a positive term $\sum_{r,h,u} [C_{Eqr} - C_{Eqh}]_+^2 \cdot X_{qu}[C_{Equ} - C_{Eqr}]_+$. However, for each positive $[C_{Eqr} - C_{Eqh}]_+^2 \cdot X_{qu}[C_{Equ} - C_{Eqr}]_+$, there always exists one and only one negative term $[C_{Equ} - C_{Eqh}]_+^2 \cdot \{-X_{qu}[C_{Equ} - C_{Eqr}]_+\}$, such that

$$\begin{aligned} & [C_{Eqr}(X_{qr}(t)) - C_{Eqh}(X_{qh}(t))]_+^2 \cdot X_{qu}[C_{Equ}(X_{qu}(t)) \\ & - C_{Eqr}(X_{qr}(t))]_+ + [C_{Equ}(X_{qu}(t)) - C_{Eqh}(X_{qh}(t))]_+^2 \\ & \cdot \{-X_{qu}[C_{Equ}(X_{qu}(t)) - C_{Eqr}(X_{qr}(t))]_+\} < 0. \quad (57) \end{aligned}$$

Hence if \mathbf{X} is not an equilibrium, $\text{grad } V(\mathbf{X}) \cdot \Delta(\mathbf{X}(t)) < 0$ is proved. In this case, according to Theorem 4, if the total travel cost $C_E(\cdot)$ is continuously differentiable and is an increasing function, for any starting point $X_0 \in \mathbf{D} \times \mathbf{F} \cap \mathbf{S}$, the dynamic system in (24) is stable.

Theorem 5 is proved.

APPENDIX C PROOF OF THEOREM 8

In this appendix, we shall prove that $\frac{\partial V(\mathbf{X}(t), \mathbf{G}(t))}{\partial \mathbf{X}(t)} \cdot \Delta \mathbf{X}(t) + \frac{\partial V(\mathbf{X}(t), \mathbf{G}(t))}{\partial \mathbf{G}(t)} \cdot \Delta \mathbf{G}(t) < 0$, for all non-equilibrium $[\mathbf{X}(t), \mathbf{G}(t)]$ in $\mathbf{D} \times \mathbf{F} \cap (\cup \mathbf{S}_i)$. Under the circumstance that a new equilibrium is in the feasible region, $\frac{\partial V(\mathbf{X}(t), \mathbf{G}(t))}{\partial \mathbf{X}(t)} \cdot \Delta \mathbf{X}(t)$ can be expressed as (58), shown at the bottom of the page, where \mathbf{J}_{qXrh} is equal to \mathbf{J}_{qrh} in Appendix B.

As proved in Appendix B, for all non-equilibrium vector $[\mathbf{X}(t), \mathbf{G}(t)]$, each $\Delta_{\text{ODq}}^{\text{T}}(\mathbf{X}(t)) \cdot \mathbf{J}_{\text{qXrh}} \cdot \Delta_{\text{ODq}}(\mathbf{X}(t))$ and $\sum_{r,h,u} \{[C_{Eqr}(X_{qr}(t)) - C_{Eqh}(X_{qh}(t))]_+^2 \cdot \{X_{qu}[C_{Equ}(X_{qu}(t)) - C_{Eqr}(X_{qr}(t))]_+ - X_{qr}[C_{Eqr}(X_{qr}(t)) - C_{Equ}(X_{qu}(t))]_+\}\}$ are less than 0. As for the term $\Delta_{\text{ODq}}^{\text{T}}(\mathbf{G}(t)) \cdot \mathbf{J}_{\text{qXrh}} \cdot \Delta_{\text{ODq}}(\mathbf{X}(t))$, as indicated in subsection IV-B, after an incident occurring on a link,

the travel cost of the routes incorporating the incident link increases suddenly. Then the traffic flow on incident routes will swap to the other normal routes gradually. Letting k_1 be the number of routes with incident effect and k_2 be the number of normal routes. $\Delta_{\text{ODq}}^{\text{T}}(\mathbf{G}(t)) \cdot \mathbf{J}_{\text{qXrh}} \cdot \Delta_{\text{ODq}}(\mathbf{X}(t))$ can be expressed as (59), shown at the bottom of the page.

If $v = u$,

$$\begin{aligned} \Delta_{\text{ODq}}^{\text{T}}(\mathbf{G}) \cdot \mathbf{J}_{\text{qXrh}} \cdot \Delta_{\text{ODq}}(\mathbf{X}) &= \sum_{i=1}^{k_1} \left\{ \sum_{u=1}^{k_2} w' w \cdot G_{qu}[C_{Eqi} \right. \\ & - C_{Equ}]_+ \cdot X_{qi} [C_{Eqi} - C_{Equ}]_+ \\ & \cdot \left(-2 \frac{\partial C_{Equ}}{\partial X_{qu}} - 2 \frac{\partial C_{Eqi}}{\partial X_{qi}} \right) \Big\}, \quad (60) \end{aligned}$$

which is less than 0.

If $v \neq u$,

$$\begin{aligned} \Delta_{\text{ODq}}^{\text{T}}(\mathbf{G}) \cdot \mathbf{J}_{\text{qXrh}} \cdot \Delta_{\text{ODq}}(\mathbf{X}) &= \sum_{i=1}^{k_1} \left\{ \sum_{u=1}^{k_2} w' w \cdot G_{qu}[C_{Eqi} \right. \\ & - C_{Equ}]_+ \cdot X_{qi} [C_{Eqi} - C_{Equ}]_+ \\ & \cdot \left(-2 \frac{\partial C_{Eqi}}{\partial X_{qi}} \right) \Big\}, \quad (61) \end{aligned}$$

which is also less than 0. Hence $\Delta_{\text{ODq}}^{\text{T}}(\mathbf{G}(t)) \cdot \mathbf{J}_{\text{qXrh}} \cdot \Delta_{\text{ODq}}(\mathbf{X}(t)) < 0$ and $\frac{\partial V(\mathbf{X}(t), \mathbf{G}(t))}{\partial \mathbf{X}(t)} \cdot \Delta \mathbf{X}(t) < 0$.

Then, if $\frac{\partial V(\mathbf{X}(t), \mathbf{G}(t))}{\partial \mathbf{G}(t)} \cdot \Delta \mathbf{G}(t)$ is also less than 0, according to Theorem 4, under the circumstance that the new equilibrium is in the feasible region, the system is stable. $\frac{\partial V(\mathbf{X}(t), \mathbf{G}(t))}{\partial \mathbf{G}(t)} \cdot \Delta \mathbf{G}(t)$ can be written as

$$\begin{aligned} \frac{\partial V(\mathbf{X}, \mathbf{G})}{\partial \mathbf{G}} \cdot \Delta \mathbf{G} &= \sum_q \{ 2 \Delta_{\text{ODq}}^{\text{T}}(\mathbf{X}) \cdot \mathbf{J}_{\text{qGrh}} \cdot \Delta_{\text{ODq}}(\mathbf{G}) \\ & + w'^2 \sum_{r,h,u} \{ [C_{Eqh} - C_{Eqr}]_+^2 \cdot \{ G_{qr}[C_{Equ} \\ & - C_{Eqr}]_+ - G_{qu}[C_{Eqr} - C_{Equ}]_+ \} \} \\ & + 2 \Delta_{\text{ODq}}^{\text{T}}(\mathbf{G}) \cdot (-\mathbf{J}_{\text{qGrh}}) \cdot \Delta_{\text{ODq}}(\mathbf{G}) \}. \quad (62) \end{aligned}$$

$$\begin{aligned} \text{grad } V(\mathbf{X}) \cdot \Delta(\mathbf{X}(t)) &= \sum_q 2 \Delta_{\text{ODq}}^{\text{T}}(\mathbf{X}(t)) \mathbf{J}_{\text{qrh}} \Delta_{\text{ODq}}(\mathbf{X}(t)) + w^2 \sum_{r,h,u} \{ [C_{Eqr}(X_{qr}(t)) - C_{Eqh}(X_{qh}(t))]_+^2 \\ & \cdot [X_{qu}[C_{Equ}(X_{qu}(t)) - C_{Eqr}(X_{qr}(t))]_+ - X_{qr}[C_{Eqr}(X_{qr}(t)) - C_{Equ}(X_{qu}(t))]_+ \}, \quad (56) \end{aligned}$$

$$\begin{aligned} \frac{\partial V(\mathbf{X}(t), \mathbf{G}(t))}{\partial \mathbf{X}(t)} \cdot \Delta \mathbf{X}(t) &= \sum_q \{ 2 \Delta_{\text{ODq}}^{\text{T}}(\mathbf{X}(t)) \cdot \mathbf{J}_{\text{qXrh}} \cdot \Delta_{\text{ODq}}(\mathbf{X}(t)) + w^2 \sum_{r,h,u} \{ [C_{Eqr}(X_{qr}(t)) - C_{Eqh}(X_{qh}(t))]_+^2 \\ & \cdot [X_{qu}[C_{Equ}(X_{qu}(t)) - C_{Eqr}(X_{qr}(t))]_+ - X_{qr}[C_{Eqr}(X_{qr}(t)) - C_{Equ}(X_{qu}(t))]_+ \} \\ & + 2 \Delta_{\text{ODq}}^{\text{T}}(\mathbf{G}(t)) \cdot (-\mathbf{J}_{\text{qXrh}}) \cdot \Delta_{\text{ODq}}(\mathbf{X}(t)) \}. \quad (58) \end{aligned}$$

$$\begin{aligned} \Delta_{\text{ODq}}^{\text{T}}(\mathbf{G}(t)) \cdot \mathbf{J}_{\text{qXrh}} \cdot \Delta_{\text{ODq}}(\mathbf{X}(t)) &= \sum_{i=1}^{k_1} \left\{ \sum_{u=1}^{k_2} w' \{ G_{qu}[C_{Eqi}(X_{qi}(t)) - C_{Equ}(X_{qu}(t))]_+ \right. \\ & \cdot [0, \dots, 0, \underbrace{-2 \frac{\partial C_{Equ}(X_{qu}(t))}{\partial X_{qu}(t)}}_{u-th}, 0, \underbrace{2 \frac{\partial C_{Eqi}(X_{qi}(t))}{\partial X_{qi}(t)}}_{i-th}, 0, \dots, 0] \\ & \cdot \sum_{v=1}^{k_2} w \{ X_{qi} [C_{Eqi}(X_{qi}(t)) - C_{Eqv}(X_{qv}(t))]_+ \Delta_{qiv} \}. \quad (59) \end{aligned}$$

As $C_{Eqr}(G_{qr}(t))$ is a decreasing function, the matrix \mathbf{J}_{qGrh} is a semi-positive definite matrix. Following the same procedure as that in the proof of $\frac{\partial V(\mathbf{X}(t), \mathbf{G}(t))}{\partial \mathbf{X}(t)} \cdot \Delta \mathbf{X}(t) < 0$, it can be readily shown that $\frac{\partial V(\mathbf{X}(t), \mathbf{G}(t))}{\partial \mathbf{G}(t)} \cdot \Delta \mathbf{G}(t) < 0$. Conclusion readily follows that the system is stable when the new equilibrium is in the feasible region.

However, under the circumstance that the new equilibrium lies outside the feasible region, the green-time proportion change can be written as (42) and (41). In this case,

$$\begin{aligned} & \frac{\partial V(\mathbf{X}, \mathbf{G})}{\partial \mathbf{X}} \cdot \Delta \mathbf{X} \\ &= \sum_q \{2\Delta^T(\mathbf{X}) \cdot \mathbf{J} \cdot \Delta(\mathbf{X}) + w^2 \sum_{r,h,u} \{[C_{Eqr} - C_{Eqh}] \cdot \{X_{qu} [C_{Equ} - C_{Eqr}]_+ - X_{qr} [C_{Eqr} - C_{Equ}]_+\} + 2\Delta^T(\mathbf{G}) \cdot \mathbf{J} \cdot \Delta(\mathbf{X})\}, \end{aligned} \quad (63)$$

which can be shown to be less than 0 according to the proof of (58). Moreover,

$$\begin{aligned} & \frac{\partial V(\mathbf{X}, \mathbf{G})}{\partial \mathbf{G}} \cdot \Delta \mathbf{G} \\ &= \sum_q \{2\Delta^T(\mathbf{X}) \cdot \mathbf{J} \cdot \Delta(\mathbf{G}) + w^2 \sum_{r,h,u} \{[C_{Eqh} - C_{Eqr}]_+^2 \cdot \{G_{qr} [C_{Equ} - C_{Eqr}]_+ - G_{qu} [C_{Eqr} - C_{Equ}]_+\} + 2\Delta^T(\mathbf{G}) \cdot \mathbf{J} \cdot \Delta(\mathbf{G})\}, \end{aligned} \quad (64)$$

where $w^2 \sum_{r,h,u} \{[C_{Eqh} - C_{Eqr}]_+^2 \cdot \{G_{qr} [C_{Equ} - C_{Eqr}]_+ - G_{qu} [C_{Eqr} - C_{Equ}]_+\}$ is proved to be less than 0, for all non-equilibrium $\mathbf{X}(t), \mathbf{G}(t)$, as indicated in Appendix B. However, because the matrix \mathbf{J}_{qGrh} is a semi-positive definite matrix, $\Delta_{ODq}^T(\mathbf{G}(t)) \cdot \mathbf{J}_{qGrh} \cdot \Delta_{ODq}(\mathbf{G}(t))$ is greater than 0 and $\Delta_{ODq}^T(\mathbf{X}(t)) \cdot \mathbf{J}_{qGrh} \cdot \Delta_{ODq}(\mathbf{G}(t))$ can be also proved to be greater than 0 according to the same procedure as that in the proof of (62). In this case, considering both (63) and (64), if the route flow \mathbf{X} and green-time proportion \mathbf{G} can meet the sufficient condition that

$$\begin{aligned} & \Delta_{ODq}^T(\mathbf{X}(t)) \cdot \mathbf{J}_{qXrh} \cdot \Delta_{ODq}(\mathbf{X}(t)) \\ & + \Delta_{ODq}^T(\mathbf{G}(t)) \cdot \mathbf{J}_{qXrh} \cdot \Delta_{ODq}(\mathbf{X}(t)) \\ & + \Delta_{ODq}^T(\mathbf{G}(t)) \cdot \mathbf{J}_{qGrh} \cdot \Delta_{ODq}(\mathbf{G}(t)) \\ & + \Delta_{ODq}^T(\mathbf{X}(t)) \cdot \mathbf{J}_{qGrh} \cdot \Delta_{ODq}(\mathbf{G}(t)) < 0, \end{aligned} \quad (65)$$

then $\frac{\partial V(\mathbf{X}(t), \mathbf{G}(t))}{\partial \mathbf{X}(t)} \cdot \Delta \mathbf{X}(t) + \frac{\partial V(\mathbf{X}(t), \mathbf{G}(t))}{\partial \mathbf{G}(t)} \cdot \Delta \mathbf{G}(t)$ can be proved to be less than 0.

The sufficient condition in (65) can be presented as two conditions that for each route i of all OD pairs, 1) $\frac{\partial C_{Ei}(X_i(t))}{\partial X_i(t)} + \frac{\partial C_{Ei}(G_i(t))}{\partial G_i(t)} > 0$; and 2) $wX_i > w'G_i$. If both conditions are satisfied, $\frac{\partial V(\mathbf{X}(t), \mathbf{G}(t))}{\partial \mathbf{X}(t)} \cdot \Delta \mathbf{X}(t) + \frac{\partial V(\mathbf{X}(t), \mathbf{G}(t))}{\partial \mathbf{G}(t)} \cdot \Delta \mathbf{G}(t) < 0$ and the system in (43) is stable when the new equilibrium is outside the feasible region.

Theorem 7 is proved.

REFERENCES

- [1] *Benefits of Traffic Incident Management*, National Traffic Incident Management Coalition, Amer. Assoc. State Highway Transp. Officials, Washington, DC, USA, 2007.
- [2] H. Park, A. Shafahi, and A. Haghani, "A stochastic emergency response location model considering secondary incidents on freeways," *IEEE Trans. Intell. Transp. Syst.*, vol. 17, no. 9, pp. 2528–2540, Sep. 2016.
- [3] B. Ghosh, M. T. Asif, J. Dauwels, U. Fastenrath, and H. Guo, "Dynamic prediction of the incident duration using adaptive feature set," *IEEE Trans. Intell. Transp. Syst.*, vol. 20, no. 11, pp. 4019–4031, Nov. 2019.
- [4] D. Schrank and T. Lomax, *2007 Urban Mobility Report*, Texas Transp. Inst., Texas A&M Univ., College Station, TX, USA, 2007.
- [5] S. Thajchayapong and J. A. Barria, "Spatial inference of traffic transition using Micro–Macro traffic variables," *IEEE Trans. Intell. Transp. Syst.*, vol. 16, no. 2, pp. 854–864, Apr. 2015.
- [6] J. Wang, X. Li, S. S. Liao, and Z. Hua, "A hybrid approach for automatic incident detection," *IEEE Trans. Intell. Transp. Syst.*, vol. 14, no. 3, pp. 1176–1185, Sep. 2013.
- [7] J. A. Barria and S. Thajchayapong, "Detection and classification of traffic anomalies using microscopic traffic variables," *IEEE Trans. Intell. Transp. Syst.*, vol. 12, no. 3, pp. 695–704, Sep. 2011.
- [8] S. Thajchayapong, E. S. Garcia-Trevino, and J. A. Barria, "Distributed classification of traffic anomalies using microscopic traffic variables," *IEEE Trans. Intell. Transp. Syst.*, vol. 14, no. 1, pp. 448–458, Mar. 2013.
- [9] E. D'Andrea, P. Ducange, B. Lazerini, and F. Marcelloni, "Real-time detection of traffic from Twitter stream analysis," *IEEE Trans. Intell. Transp. Syst.*, vol. 16, no. 4, pp. 2269–2283, Aug. 2015.
- [10] C. Zhan, A. Gan, and M. Hadi, "Prediction of lane clearance time of freeway incidents using the M5P tree algorithm," *IEEE Trans. Intell. Transp. Syst.*, vol. 12, no. 4, pp. 1549–1557, Dec. 2011.
- [11] X. Ma, C. Ding, S. Luan, Y. Wang, and Y. Wang, "Prioritizing influential factors for freeway incident clearance time prediction using the gradient boosting decision trees method," *IEEE Trans. Intell. Transp. Syst.*, vol. 18, no. 9, pp. 2303–2310, Sep. 2017.
- [12] J. Long, Z. Gao, P. Orenstein, and H. Ren, "Control strategies for dispersing incident-based traffic jams in two-way grid networks," *IEEE Trans. Intell. Transp. Syst.*, vol. 13, no. 2, pp. 469–481, Jun. 2012.
- [13] Y.-S. Huang, Y.-S. Weng, and M. Zhou, "Design of traffic safety control systems for emergency vehicle preemption using timed Petri nets," *IEEE Trans. Intell. Transp. Syst.*, vol. 16, no. 4, pp. 2113–2120, Aug. 2015.
- [14] L. Qi, M. Zhou, and W. Luan, "Emergency traffic-light control system design for intersections subject to accidents," *IEEE Trans. Intell. Transp. Syst.*, vol. 17, no. 1, pp. 170–183, Jan. 2016.
- [15] M. Smith, "Traffic signal control and route choice: A new assignment and control model which designs signal timings," *Transp. Res. C, Emerg. Technol.*, vol. 58, pp. 451–473, Sep. 2015.
- [16] J. Wardrop and J. I. Whitehead, "Correspondence. some theoretical aspects of road traffic research," *ICE Proc. Eng. Divisions*, vol. 1, no. 5, pp. 767–768, 1952.
- [17] M. Smith and R. Mounce, "A splitting rate model of traffic re-routings and traffic control," *Transp. Res. B, Methodol.*, vol. 45, no. 9, pp. 1389–1409, Nov. 2011.
- [18] S. Lin, Q.-J. Kong, and Q. Huang, "A simulation analysis on the existence of network traffic flow equilibria," *IEEE Trans. Intell. Transp. Syst.*, vol. 15, no. 4, pp. 1706–1713, Aug. 2014.
- [19] L. Chen and T. Hu, "Flow equilibrium under dynamic traffic assignment and signal control—An illustration of pretimed and actuated signal control policies," *IEEE Trans. Intell. Transp. Syst.*, vol. 13, no. 3, pp. 1266–1276, Sep. 2012.
- [20] X. He, X. Guo, and H. X. Liu, "A link-based day-to-day traffic assignment model," *Transp. Res. B, Methodol.*, vol. 44, no. 4, pp. 597–608, May 2010.
- [21] X. Zhao, C. Wan, H. Sun, D. Xie, and Z. Gao, "Dynamic rerouting behavior and its impact on dynamic traffic patterns," *IEEE Trans. Intell. Transp. Syst.*, vol. 18, no. 10, pp. 2763–2779, Oct. 2017.
- [22] M. Smith, R. Liu, and R. Mounce, "Traffic control and route choice: Capacity maximisation and stability," *Transp. Res. B, Methodol.*, vol. 81, pp. 863–885, Nov. 2015.
- [23] S. Wang, C. Li, W. Yue, and G. Mao, "Network capacity maximization using route choice and signal control with multiple OD pairs," *IEEE Trans. Intell. Transp. Syst.*, vol. 21, no. 4, pp. 1595–1611, Apr. 2020.
- [24] L. Armijo, "Minimization of functions having Lipschitz continuous first partial derivatives," *Pacific J. Math.*, vol. 16, no. 1, pp. 1–3, 1966.
- [25] W. Bischof, "Analysis of $M/G/1$ -Queues with setup times and vacations under six different service disciplines," *Queueing Syst.*, vol. 39, no. 4, pp. 265–301, 2001.
- [26] T. Van Woensel and N. Vandaele, "MODELING TRAFFIC FLOWS WITH QUEUEING MODELS: A REVIEW," *Asia-Pacific J. Oper. Res.*, vol. 24, no. 04, pp. 435–461, Aug. 2007.

- [27] M. Baykal-Gürsoy, W. Xiao, and K. Ozbay, "Modeling traffic flow interrupted by incidents," *Eur. J. Oper. Res.*, vol. 195, no. 1, pp. 127–138, May 2009.
- [28] *Lyapunov Stability*. Accessed: Nov. 24, 2019. [Online]. Available: https://en.wikipedia.org/wiki/Lyapunov_stability
- [29] G. Guo and P. Zhang, "Asymptotic stabilization of USVs with actuator dead-zones and yaw constraints based on fixed-time disturbance observer," *IEEE Trans. Veh. Technol.*, vol. 69, no. 1, pp. 302–316, Jan. 2020.
- [30] R. Jain and J. M. Smith, "Modeling vehicular traffic flow using M/G/C/C state dependent queueing models," *Transp. Sci.*, vol. 31, no. 4, pp. 324–336, Nov. 1997.
- [31] A. Lyapunov, "The general problem of the stability of motion," Ph.D. dissertation, Kharkiv Math. Soc., Univ. Kharkiv, Kharkiv, Ukraine, 1892.
- [32] J. Wang and H. Niu, "A distributed dynamic route guidance approach based on short-term forecasts in cooperative infrastructure-vehicle systems," *Transp. Res. D, Transp. Environ.*, vol. 66, pp. 23–34, Jan. 2019.
- [33] Y.-C. Chiu and N. Huynh, "Location configuration design for dynamic message signs under stochastic incident and ATIS scenarios," *Transp. Res. C, Emerg. Technol.*, vol. 15, no. 1, pp. 33–50, Feb. 2007.



Wenwei Yue (Student Member, IEEE) received the B.E. degree in information engineering from Xidian University, China, in 2015, where he is currently pursuing the Ph.D. degree in communication and information systems. He is also a visiting Ph.D. student with the School of Computing and Communications, University of Technology Sydney, from February 2017 to February 2019. His current research interests include intelligent transportation systems, vehicular networks, and big data.



Changle Li (Senior Member, IEEE) received the Ph.D. degree in communication and information system from Xidian University, China, in 2005. He conducted his Post-Doctoral Research in Canada and the National Institute of Information and Communications Technology, Japan, respectively. He had been a Visiting Scholar with the University of Technology Sydney. He is currently a Professor with the State Key Laboratory of Integrated Services Networks, Xidian University. His research interests include intelligent transportation systems, vehicular networks, mobile ad-hoc networks, and wireless sensor networks.



Shangbo Wang (Member, IEEE) received the Dr.-Ing. degree from the University of Duisburg-Essen, Germany, and the Ph.D. degree from the University of Technology Sydney. He was with Siemens AG, Munich, Germany, and Continental AG, Germany, as a Research Scientist and a Research Engineer, respectively. He is currently working as a Research Fellow with The University of Sydney. He is also a qualified Academic Researcher and an Engineer in intelligent transportation systems, applied mathematics, data analysis, machine learning, and wireless communication. He is with many years of research experience in data analysis, statistics and machine learning, wireless communication, signal processing, and software development.



Zhigang Xu (Member, IEEE) received the B.S. degree in automation and the M.S. and Ph.D. degrees in traffic information engineering and control from Chang'an University, China, in 2002, 2005, and 2012, respectively. He is currently a Professor with the School of Information Engineering, and the Director of the Lab of Traffic Information Sensing and Control, Chang'an University. He had worked with the University of California at Davis, Davis, CA, USA, as a Visiting Scholar in 2015. His research focuses on connected and autonomous vehicles, traffic flow analysis, transportation optimization, and intelligent transportation systems. He is also the Chair of CAVs Committee of World Transportation Convention and a member of the IEEE ITS society and ASCE.



Guoqiang Mao (Fellow, IEEE) has published more than 200 papers in international conferences and journals, which have been cited more than 9000 times. His research interests include intelligent transport systems, applied graph theory and its applications in telecommunications, the Internet of Things, wireless sensor networks, wireless localization techniques and network modeling, and performance analysis. He is a fellow of IET. He received Top Editor Award for outstanding contributions to the IEEE TRANSACTIONS ON VEHICULAR TECHNOLOGY in 2011, 2014, and 2015. He was the Co-Chair of the IEEE Intelligent Transport Systems Society Technical Committee on Communication Networks. He has served as a chair, the co-chair, and a TPC member in a number of international conferences. He was an Editor of the IEEE TRANSACTIONS ON WIRELESS COMMUNICATIONS from 2014 to 2019. He has been an Editor of the IEEE TRANSACTIONS ON VEHICULAR TECHNOLOGY since 2010 and the IEEE TRANSACTIONS ON INTELLIGENT TRANSPORTATION SYSTEMS since 2018.